CATÓLICA
ESCOLA SUPERIOR DE BIOTECNOLOGIA
PORTO

THE EFFECT OF CADMIUM ON THE NET N_2O PRODUCTION OF DEEP-SEA BACTERIA

by Leonor Pizarro Mendes

October 2022

CATÓLICA
ESCOLA SUPERIOR DE BIOTECNOLOGIA
PORTO

THE EFFECT OF CADMIUM ON THE NET N_2O PRODUCTION OF DEEP-SEA BACTERIA

Thesis presented to *Escola Superior de Biotecnologia* of the *Universidade Católica Portuguesa* to fulfill the requirements of Master of Science degree in Applied Microbiology

by

Leonor Pizarro Mendes

Supervisor: Dr. Miguel Semedo

Co-Supervisors: Dr. Catarina Magalhães; Dr. Maria de Fátima Carvalho

Tutor (University): Dr. Irina Moreira

October 2022

Resumo

As bactérias do mar profundo têm grande importância ambiental, devido ao seu papel ativo no ciclo dos nutrientes, entre outras atividades. Algumas destas bactérias são responsáveis pela manutenção de baixos níveis naturais de óxido nitroso (N_2O), um poderoso gás com efeito de estufa, reduzindo-o a azoto molecular gasoso (N_2), através da via de desnitrificação.

Paralelamente, o aumento da mineração do fundo dos oceanos pode aumentar a exposição das bactérias marinhas a concentrações tóxicas de metais, tais como cádmio e chumbo, e outros elementos raros. Contudo, a suscetibilidade da via redutora de N_2O à exposição a metais é relativamente desconhecida, sobretudo em condições de mar profundo.

O objetivo desta dissertação é compreender os potenciais impactos da exposição ao cádmio no fluxo de N_2O por bactérias do mar profundo, utilizando como modelo *Shewanella loihica* PV-4, uma estirpe tolerante à pressão e com potencial genético para produzir e remover N_2O.

As experiências de exposição ao cádmio foram realizadas de forma a permitir o crescimento aeróbico de *S. loihica* PV-4 dentro dos biorreatores através da manutenção de um fluxo de ar sintético. Quando o crescimento atingiu a fase exponencial média ou tardia, o fluxo de gás foi alterado para N_2, no sentido de estimular as condições de desnitrificação. Nesta fase de anóxia, foi feita amostragem do ar dentro dos biorreatores em sete pontos ao longo do tempo para quantificar a acumulação de N_2O, e foram recolhidas também quatro amostras de cultura ao longo do tempo para extração de RNA de forma a avaliar as expressões relativas dos genes *nirK* e *nosZ*, essenciais na produção e redução de N_2O, respetivamente.

Na experiência de exponencial média, o fluxo de N_2O apresentou um valor de 2,307 ± 1,428 ppm/min no controlo e zero para o tratamento com cádmio. O rácio *nirK/nosZ* do controlo foi 10 vezes superior ao do tratamento com cádmio ($nirK/nosZ_{\text{CÁDMIO}}$ = 1,384; $nirK/nosZ_{\text{CONTROLO}}$ = 13,415), consistente com o fluxo positivo de N_2O neste tratamento. Nesta fase de crescimento, a via metabólica de desnitrificação parece estimular a produção de N_2O. Na experiência de exponencial tardia, os fluxos de N_2O foram zero para ambos os tratamentos. Contudo, os níveis de fundo de N_2O no tratamento com cádmio revelaram-se mais elevados do que no controlo. Ao contrário do que aconteceu na exponencial-média, na exponencial tardia, a expressão relativa de *nosZ* foi mais elevada que *nirK* em ambos os tratamentos ($nirK/nosZ_{\text{CÁDMIO}}$ = 0,008; $nirK/nosZ_{\text{CONTROLO}}$ = 0,007), o que é consistente com a ausência de fluxos de N_2O. Apesar das diferenças de resposta entre a fase exponencial média e tardia, é possível perceber que o cádmio pode afetar o processo de desnitrificação em *S. loihica* PV-4.

Palavras-chave: óxido nitroso; mar profundo; desnitrificação; *Shewanella*

Abstract

Deep-sea bacteria have high environmental importance due to their active role on nutrient cycling, among other activities. Some of these bacteria are responsible for maintaining low natural levels of nitrous oxide (N_2O), a powerful greenhouse gas and ozone-depleting, by reducing it to dinitrogen gas (N_2), through the denitrification pathway. The growth of deep-sea mining activities may increase the exposure of marine bacteria to toxic concentrations of metals such as cadmium and lead, as well as other rare elements. However, the susceptibility of the N_2O-reducing pathway to metal exposure is relatively unknown, especially in deep-sea conditions.

The aim of this dissertation is to understand potential impacts of cadmium exposure on net N_2O production, by deep-sea bacteria. For this, we used mostly the strain *Shewanella loihica* PV-4 as a model, a piezotolerant deep-sea isolate with genetic potential to produce and remove N_2O. Cadmium exposure experiments started with synthetic air flowing to allow *S. loihica* PV-4 aerobic growth inside closed bioreactors. When growth reached mid or late exponential phase, gas supply was changed to N_2 to create an anoxic environment towards stimulating denitrifying conditions. Headspace gas sampling was performed at seven time points during anoxia to quantify N_2O accumulation. Over the same period of time, four liquid culture samples were taken for RNA extraction to assess *nirK* and *nosZ* relative expression, two key genes for net N_2O production.

In the mid-exponential experiment, net N_2O production showed a positive flux of 2,307 ± 1,428 ppm/min in the control and a null flux for cadmium treatment. For the control treatment, the ratio *nirK/nosZ* was 10x times higher than in the cadmium treatment ($nirK/nosZ_{CADMIUM}$ = 1,384; $nirK/nosZ_{CONTROL}$ = 13,415), supporting the positive flux in this treatment. In the late-exponential experiment, net N_2O production fluxes were zero for both treatments, but the background levels of N_2O in the cadmium treatment were higher than in the control. Relative expression of *nosZ* was much higher than *nirK* ($nirK/nosZ_{CADMIUM}$ = 0,008; $nirK/nosZ_{CONTROL}$ = 0,007) in the late-exponential stage, explaining the low N_2O values quantified in both treatments, when compared to the mid-exponential.

Either in the mid-exponential experiment, where cadmium appears to inhibit net N_2O production, or in the late-exponential experiment, where cadmium might increase N_2O production, this implies that the nitrogen cycle can be altered by cadmium exposure in marine environments.

Keywords: nitrous oxide; deep-sea; denitrification; *Shewanella*

Acknowledgments

I would like to thank my supervisor, Dr. Miguel Semedo, whose knowledge and insight guided me through this past year. His constant support and dedicated guidance, along with some patience and a lot of enthusiasm for this research steered me through what I can call a great year in my academic life.

Also, I would like to thank my co-supervisors Dr. Catarina Magalhães and Dr. Maria de Fátima Carvalho for all the advice and support during this research. I wish to extend my thanks my colleagues from EcoBioTec laboratory, at Centro Interdisciplinar de Investigação Marinha e Ambiental – CIIMAR, that always helped me when needed and made me feel welcome.

I would also like to thank all my professors at Escola Superior de Biotecnologia for helping me build the foundations that made this year possible.

And lastly, I would like to truly thank my family and friends for all the support and encouragement. I simply couldn't have done this without them.

This research is comprised in the MIDFun project. This project has received funding from the European Union's Horizon 2020 research and innovation programme under the Marie Skłodowska-Curie grant agreement No 101038095. This research also had the support of the BYT+ program, a student grant from "Verão com Ciência 2022" funded by FCT, and partial support from the project N-MICROARCTIC (2022.02983.PTDC).

Contents

Introduction

Deep-sea bacteria and the N cycle

Deep-sea bacteria have major environmental and overall importance, as high biodiverse communities play significant roles on organic matter remineralization, energy transfer, and nutrient cycling (Mason *et al.*, 2009), and are a potential source of novel natural products (Saide, Lauritano and Ianora, 2021).

Ocean's nitrogen (N) cycle (Figure 1) accounts for several biogeochemical microbial transformations (Hutchins and Capone, 2022).

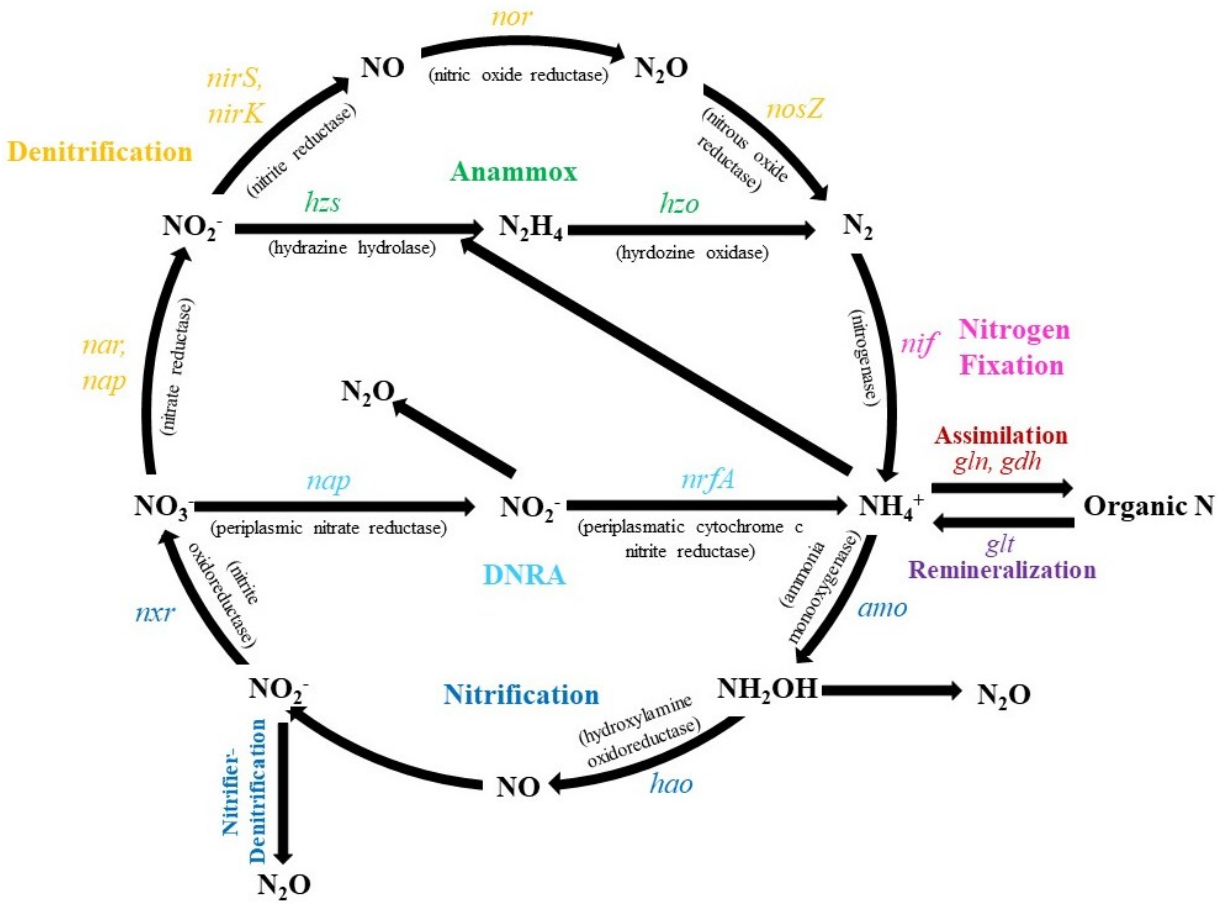

Figure 1: Nitrogen cycle processes, pathways, enzymes, and genes. The arrows show pathways, between parenthesis are the enzymes responsible for that pathway, and next to them in italic are the genes. Processes and their corresponding enzymes are colored the same: denitrification (*nar, nap, nirS/nirK, nor*, *nosZ*) in yellow; nitrogen fixation (*nif*) in magenta; ammonium assimilation (*gln, gdh*) in bordeaux; nitrogen remineralization (*glt*) in purple; nitrification (*amo, hao, nxr*) and nitrifier-denitrification in dark blue; DNRA (*nap, nrfA*) in light blue; and annamox (*hzs, hzo*) in green. *Notes: DNRA – dissimilatory nitrate reduction to ammonia, also known as respiratory ammonification; Anammox - anaerobic ammonium oxidation.*

Adapted from Hallin *et al.* (2017) and Pajares and Ramos (2019).

These numerous biogeochemical processes mediated by microorganisms are responsible for driving the marine N cycle. These processes include those that contribute to the marine fixed nitrogen (N_2 fixation), to retained nitrogen (nitrification, assimilation, and dissimilatory nitrate reduction to ammonia [DNRA]), along with those that contribute to the nitrogen loss (denitrification, anaerobic ammonium oxidation [Annamox] and nitrite-dependent anaerobic methane oxidation) (Pajares and Ramos, 2019).

External factors also affect the responses of these microorganisms, consequently affecting the N processes. These factors can include oxygen availability, pH, light, temperature, and inorganic N availability like ammonium, nitrate and nitrite (Pajares and Ramos, 2019). For example, anoxic conditions are favorable for bacterial denitrification (Stein, 2011; Battaglia and Joos, 2018), and ocean acidification may cause a decline in nitrification rates (Pajares and Ramos, 2019). As this is a cycle, every process is interconnected. Taking the last example, the decreasing of nitrification rates might lower availability of nitrite (NO_2^-) or nitrate (NO_3^-) for further processes, such as DNRA, denitrification and anammox.

Taking the interconnectivity into account, we can imagine that new external factors could impact the marine N cycle processes by influencing microbial responses, that in a large scale it potentially impacts greenhouse gases regulation, as nitrous oxide (N_2O) is a powerful greenhouse gas that can be release in some of the N cycle pathways.

Nitrous oxide

Nitrous oxide (N_2O) is a strong greenhouse gas and ozone-depleting substance (Freing, Wallace and Bange, 2012), with a global warming potential of 273 times that of carbon dioxide (CO_2) (EPA United States Environmental Protection Agency, 2022). Despite often overlooked, N_2O is predicted to have an impact of 6% on greenhouse gas emissions (BBC, 2021). Impacts on the sources and controls of N_2O production are, therefore, of great relevance in regard to climate change and global warming.

Nitrous oxide can be released during denitrification or nitrification processes, as well as by DNRA. Essentially, important sources of atmospheric N_2O come from nitrification and denitrification in both marine and terrestrial ecosystems. Agricultural systems are substantial sources of N_2O to the environment, accounting for roughly 25% of worldwide N_2O emissions (Canfield, Glazer and Falkowski, 2010). Oceanic emissions account for 10% to 53% of natural and anthropogenic N_2O sources, a broad interval that reflects the uncertainty brought by few measurements and low control of marine N_2O (Bange *et al.*, 2019). Nitrous oxide

concentrations have high variability in the oceans, reaching ≈1500 nM in suboxic deep waters of the Baltic Sea, ≈1000 nM in coastal waters off Peru, and <1 nM in the constantly anoxic deep waters of the Black Sea and Cariaco Trench (Arévalo-Martínez *et al.*, 2015; Bange *et al.*, 2019).

The net N_2O production derives from the balance between consumption and production rates that can be rather significant. In oceanic environments, net N_2O production is driven by remineralization fluxes, O_2 concentrations, and pH (Battaglia and Joos, 2018; Breider *et al.*, 2019). For example, while N_2O produced in nitrification follows aerobic remineralization of organic matter and is dependent on oxygen consumption, N_2O produced in denitrification occurs in low oxygenated waters together with anaerobic remineralization (Battaglia and Joos, 2018). Additionally, ocean acidification is believed to potentially reduce ocean nitrification and N_2O production (Breider *et al.*, 2019).

Bacterial and archaeal N_2O reducers are thought to be the only biological sink to this gas (Kuypers, Marchant and Kartal, 2018; Semedo *et al.*, 2020). Nitrous oxide reducing bacteria are widely spread throughout a wide range of phyla (Hallin *et al.*, 2017), and are present in the deep-sea. The N_2O reducing reaction is catalyzed by N_2O reductase and generates dinitrogen gas (N_2). The enzyme N_2O reductase is encoded in the *nosZ*, a gene that is often a biomarker in studies of N_2O-reducing denitrifiers in marine systems (Pajares and Ramos, 2019).

nosZ gene carriers phylogenetically divide into two clades: clade I (nosZ-I), that mostly comprises microorganisms that hold a complete denitrification pathway, and clade II (nosZ-II), that includes most N_2O reducers that lack the other denitrification genes (Graf, Jones and Hallin, 2014; Hallin *et al.*, 2018; Semedo *et al.*, 2020). Some of these denitrification genes that lack in nosZ-II can be *nir* or *nor*, not being able to produce N_2O, indicating they are primarily N_2O consumers (Graf, Jones and Hallin, 2014). Other significant differences between clades I and II rely on nosZ-I always being flanked by a *nosR* gene, and having a twin-arginine translocation (TAT) pathway, whereas nosZ-II species are linked to the Sec translocation pathway (Hallin *et al.*, 2017). Additionally, nosZ-I and nosZ-II expression may respond differently to varying nitrogen conditions and the presence of competing electron acceptors (Semedo *et al.*, 2020). Regardless of the phylogeny of the nosZ-carrying microorganisms, N_2O production and reduction can be impacted by human activities (Semedo *et al.*, 2018; Pajares and Ramos, 2019; Orcutt *et al.*, 2020).

Deep-sea mining and environmental issues

An emerging economic activity that may impact nutrient cycle in the oceans is the deep-sea mining. Deep-sea mining has been accelerating and, with the rising demand of critical metals, it is expected to continue increasing in the future (Orcutt *et al.*, 2020). Direct impacts of deep-sea mining include the loss of natural seabed and the biodiversity it supports, compacting of the ocean floors, and the formation of sediment plumes that can disturb aquatic life. Along with having faster sedimentation rates, the nearby areas may also have lasting suspension loads that flow laterally (Sharma, 2015). The turbidity of these waters will increase as a result of a sudden rise in suspended matter brought by a sediment plume and mining waste, which can also have an impact on pelagic organisms (Sharma, 2015). Along with this, toxic metals, such as cadmium and lead, as well as other rare elements (Petersen *et al.*, 2016), can also be released in the surrounding waters by deep-sea mining activities.

It is expected that the pelagic fauna is affected by these environmental issues derived from deep-sea mining. Some of its impacts can include changes on behavior and mortality of fishes, zooplankton species, marine mammals, pelagic bacteria, and can also lead to bioaccumulation of the trace metals (Sharma, 2015). However, the effects on microbial life are currently largely unknown (Orcutt *et al.*, 2020).

Metal impacts on deep-sea bacteria

As stated above, the release of toxic concentrations of metals is a potential issue from deep-sea mining. Many microbial communities have important roles in the deep-sea, and, with this potential releasing of toxic metals, they will most likely be affected (Hauton *et al.*, 2017), along with the processes driven by them. Human activities significantly disturbs the marine N cycle (Pajares and Ramos, 2019), and metal release by deep-sea mining can be accountable for this imbalance.

Denitrification rates in aquatic environments can be considerably impacted by trace metals. Magalhães *et al.* (2007) work on estuarine sediments report that, according to the type of sediment, in addition to reducing the amount of nitrogen removed from an estuary through denitrification, trace metals can also increase the emission of N_2O. Mosier and Francis (2010) studied the denitrifier abundance and activity across the San Francisco Bay estuary, and described that metals, along with other factors, were crucial in influencing denitrification rates, *nir* abundance and community structure.

One of the most toxic metals that can be released by deep-sea mining is cadmium (Cd), which, even at low doses, is fatal to many aquatic organisms (Petersen *et al.*, 2016; Broman *et al.*, 2019). Broman *et al.* (2019) describe that cadmium can have a key role in the denitrification process in aquatic metal-polluted environments because, under hypoxic conditions, cadmium can bind to sulfide (S) and precipitate. As S has been showed to inhibit the reduction of N_2O to N_2 (Broman *et al.*, 2019), the presence of cadmium in sediments and water with sulfides might actually unlock this reduction and increase denitrification rates. However, Liu *et al.* (2016) state that elevated soil metal concentration can inhibit denitrification.

The toxicity on benthic denitrifier abundance and activity may be influenced by the bioavailability of metals and variations in the denitrifying microbial community tolerances (Mosier and Francis, 2010).

There are diverse and contrary results when it comes to cadmium impact on denitrification, but one thing is normally transverse to all: it causes an imbalance in the N cycle. However, the impacts on deep-sea N2O-reducing bacteria are currently unknown.

Dissertation objectives

The work developed for this dissertation has the objective of studying the impact of cadmium, one of the metals that might be released by deep-sea mining, on the net N_2O production by deep-bacteria. *Shewanella loihica* PV-4, a piezotolerant deep-sea isolate and *nosZ* carrier, was the strain chosen for the majority of this work, so it is the most studied and discussed in this dissertation. Other strains are referred, but not with so much extent.

The main hypothesis is that cadmium will have an impact on *S. loihica* PV-4 denitrification metabolism, leading to higher net N_2O production. To achieve the objective and test this hypothesis, several exposure experiments were performed and are presented and discussed in this dissertation.

This work, and future research on susceptibility to metal exposure by deep-sea bacteria and in deep-sea conditions, is expected to contribute to improve our understanding about the environmental risks of deep-sea mining, an anthropogenic activity that can disturb microbial communities and function.

Materials and Methods

Preliminary growth curves with a model pelagic bacterium: Ruegeria pomeroyi *DSS-3*

To later compare deep-sea isolate's growth responses to cadmium with the growth response of a pelagic bacterium, *Ruegeria pomeroyi* DSS-3 was chosen. With its whole-genome sequenced, *R. pomeroyi* DSS-3 has become a model marine bacteria, and is a representative of the Alphaproteobacteria taxon (Salgado *et al.*, 2014).

Several growth trials were performed to optimize experimental conditions. Pure cultures were aerobically grown in culture flasks of 75 cm^3 filled with 50 mL of Marine Basal Media (MBM) at 28ºC and 250 rpm agitation, in the dark, for 39 hours to 45 hours. MBM composition is: sea salts (20 g/L), 1M Tris-HCl (71,25 mL/L) with pH adjusted to 7,5 with 6N HCl, $K_2HPO_4.3H_2O$ (0,041 g/L), NH_4Cl (0,7125 g/L), and 700 mL dH_2O. The media was supplemented with glucose to a final concentration of 10 mM. Different initial inoculum percentages were tested (5%, 10%, and 30%). To measure growth, samples were taken for optical density (OD) readings at 600 nm. Incubations were finalized when the cultures appeared to reach the stationary phase of a typical bacterial growth.

After familiarization with *R. pomeroyi* DSS-3 growth, we also tried to grow the strain with higher pressure, 3 and 5 bar, in pressurized bioreactors (Bio-Xplorer 400P by H.E.L Group), to evaluate its suitability for future comparisons in near-deep-sea conditions. Control reactors were present, growing *R. pomeroyi* DSS-3 with 1 bar pressure. In this experiment, the strain grew aerobically in MBM supplemented with 10 mM glucose at 28ºC and 250 rpm agitation, with no light source. These bioreactors were filled with 200 mL of media, leaving a headspace of 200 mL. To measure growth, media samples were taken for OD readings at 600 nm. We verified no growth of *R. pomeroyi* DSS-3 under pressure, abandoning this course.

Selecting deep-sea isolates

For further investigation of N_2O metabolism within deep-sea bacteria, we selected four deep-sea isolates narrowing down a search in the DOE Joint Genome Institute – IMG database (Chen *et al.*, 2021), following the criteria: bacteria with finished genomes carrying the *nosZ* gene → marine source isolates with geographic information → isolates from deep-sea or known piezotolerants → culturable isolates → isolates available in public culture collections. Seven isolates were found matching the above criteria and the four most likely to grow faster in the

laboratory were selected: *Shewanella loihica* PV-4, *Thalassospira indica* PB8B, *Lutibacter profundi* LP1, and *Profundibacter amoris* BAR1.

S. loihica PV-4 (DSM no.: 17748, type strain), *L. profundi* LP1 (DSM no.: 100437, type strain), and *P. amoris* BAR1 (DSM no.: 104147, type strain) were obtained from DSMZ – German Collection of Microorganisms and Cell Cultures GmbH, DSM, and culture activation was done according to provided instructions. *T. indica* PB8B (strain no.: LMG 29620, type strain) was obtained from BCCM/LMG – Belgian Coordinated Collections of Microorganisms and cultivated according to provided instructions.

There is no literature information on the *nosZ*-clades of several of those seven strains. To obtain this information, we constructed a phylogenetic tree using MEGA7 software (Kumar, Stecher and Tamura, 2015). We aligned by Muscle 18 NosZ protein sequences from strains belonging to clade II and 20 from clade I, along with the NosZ sequences from the seven strains. A Maximum Likelihood phylogenetic tree was constructed with bootstrap method with 100 bootstrap replications, substitution model Jones-Taylor-Thornton, with uniform rates, and complete deletion for gaps/missing data treatment. The protein sequences of the known nosZ-I and nosZ-II were retrieved from the National Center for Biotechnology Information – NCBI (National Center for Biotechnology Information (NCBI), 1988), and the NosZ sequences from the seven strains were retrieved from DOE Joint Genome Institute – IMG database (Chen *et al.*, 2021).

Cadmium impact on bacterial growth

To select a cadmium concentration in solution for exposure experiments with *S. loihica* PV-4, its growth was studied under different dissolved concentrations of anhydrous cadmium chloride ($CdCl_2$) (Thermo Scientific Cadmium chloride, anhydrous, ACS, 99.0% min, CAS:10108-64-2). In addition, to compare cadmium sensitivity with a pelagic marine model, the same experiment was done with *R. pomeroyi* DSS-3. During the course of this dissertation research, the growth of *T. indica* PB8B, another deep-sea isolate, was also investigated under different cadmium concentrations to evaluate its potential use in future exposure experiments.

For all experiments on cadmium impact on bacterial growth, pure cultures of the three tested strains (*R. pomeroyi* DSS-3, *S. loihica* PV-4, and *T. indica* PB8B) were grown aerobically in culture flasks of 75 cm^3 filled with 50 mL of MBM at 28ºC and 250 rpm agitation, in the dark, for near 100 hours. MBM composition is described before in the section "Preliminary growth curves with a model pelagic bacterium: *Ruegeria pomeroyi* DSS-3". To the MBM media,

glucose was added as a carbon and electrons source to a final concentration of 10 mM, as well as different cadmium concentrations in solution.

Cadmium concentrations were added at five different concentrations: 0,01 mM, 0,025 mM, 0,05 mM, and 0,1 mM. These were selected based on the values of Effect Range Low (ERL = 1,2 µg/g – the concentration below which toxic effects are scarcely observed or predicted) and Effect Range Median (ERM = 9,6 µg/g – the concentration above which effects are frequently or always observed) (Long *et al.*, 1995). The higher selected metal concentration, 0,1 mM (18,3 µg/g), is placed above ERM, and the remaining are between ERL and ERM (0,01 mM = 1,8 µg/g; 0,025 mM = 4,6 µg/g; 0,05 mM = 9,2 µg/g).

Several solutions of anhydrous cadmium chloride ($CdCl_2$) with deionized water were prepared to add the same volume of solution to the inoculated flasks, achieving the final selected concentrations in the culture flasks.

To measure growth, samples were taken for optical density (OD) readings at 600 nm. Growth experiments were finalized when the cultures appeared to reach the stationary phase of a typical bacterial growth.

Cadmium effect on the net N_2O metabolism by Shewanella loihica *PV-4*

Experimental design

All cadmium exposure experiments were performed in bioreactors Bio-Xplorer 400P by HEL Group. The system is composed of 4 independent bioreactors and continuously monitors pH, dissolved oxygen (DO), temperature, pressure, and air mass flow for each individual bioreactor. To monitor bacterial growth, media samples were taken to read optical density at 600 nm in an external spectrophotometer. Culture disturbance during sample collection is minimal since a specific line and valve are used for sample collection (see Figure 3).

To minimize metabolic differences, in each experiment, the strain was picked from the same culture stock kept at -80ºC and transferred to a LB agar plate (day 0). At day 3, the growing colonies were transferred to new and more LB plates. At day 9, the cultures were ready to be retrieved from the plates and transferred to a small quantity of MBM (≈ 15 mL) to attain a dense inoculum. Agar plates were always incubated at 28ºC.

Bioreactors were filled with MBM media, 10 mM glucose, 1 mM nitrate, as electron acceptor in anoxic conditions, 0,01 mM cadmium chloride ($CdCl_2$), and 20% inoculum. Control treatments were done under the same conditions without adding $CdCl_2$. Both treatments were

replicated in individual bioreactors and in different experiments since there are only 4 reactors available in the system.

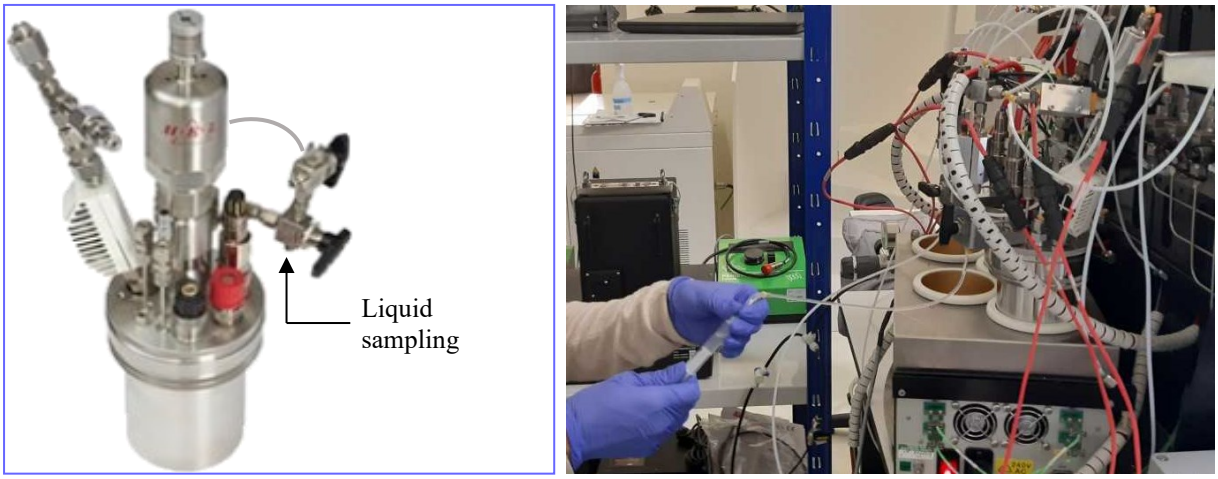

Figure 3: On the left, an image of a bioreactors Bio-Xplorer 400P by HEL Group (H.E.L Group, 2022). Liquid sampling port, where a tube can be connected to, is pointed. On the right, liquid sampling being collected.

Three similar experiments (A, B, and C) were run with the objective of attaining experimental replicates, ideally achieving 5 replicates for each treatment (1 per treatment in experiment A, 2 in experiment B, and 2 in experiment C). Only 1 replicate was used in experiment A since we tested 2 different pressure levels in this experiment (1 and 5 bar in one reactor each per treatment). Since we did not observe *S. loihica* PV-4 growth at 5 bar in experiment A, after more than 96 hours, the subsequent experiments (B and C) were only performed at 1 bar, with 2 replicates per treatment.

Experiments started with synthetic air flowing to allow *S. loihica* PV-4 aerobic growth. When growth reached mid-to-late exponential phase, gas supply was changed to N_2 to create an anoxic environment to stimulate denitrifying conditions. When the DO probe indicated an oxygen value close to zero, we started an interval gas sampling at minutes 0, 10, 20, 30, 60, 90, and 120, for further quantification of headspace N_2O. Liquid samples for RNA extraction were taken immediately before turning the flowing gas to N_2, and at minutes 10, 60 and 120 of anoxia.

Cadmium quantification

As mentioned before, the concentration of cadmium expected to be in solution for this experiment was 0,01 mM $CdCl_2$. To verify the cadmium concentration in solution, in the beginning and end of every experiment, 4 mL of the growth media were taken, centrifuged to discard the pellet, and treated with 40 µL of 68% nitric acid. Cadmium in samples was then

directly measured by atomic absorption spectrophotometry with an air-acetylene flame (AAS-flame).

To quantify the cadmium in each sample, a standard curve and linear regression with standard solutions (from 0,1 ppm to 5 ppm in experiments A and B, and from 0,025 ppm to 3 ppm in experiment C), was designed. Assessments by AAS-flame were performed in two separate moments, so there is a standard curve and linear regression for each moment.

Net N_2O production

For the gas sampling described before, 10 mL gas samples were taken using an outlet port in the bioreactors' hardware. As we took the samples, they were stored in 12 mL glass vials in vacuum, closed with rubber stopers and aluminum rings. In these gas samples, N_2O was measured and quantified within a few days after sample collection by gas chromatography coupled with electron capture detection (GC-ECD). Similar glass vials were injected with 100 ppm N_2O in the same day of collection and quantified to assure reading values of the gas samples were reliable.

Nitrous oxide results were organized in graphs relating N_2O quantity, in ppm, with time, in minutes, per treatment, per experiment. To calculate N_2O fluxes, the slope of all points for each reactor was calculated along with their square correlation coefficient (R^2). For R^2 values lower than 0,80, we consider that there is no linear relation, so the slope (and the flux) is considered null.

Gene expression

Relative expression of *nosZ* and *nirK* genes were measured by real-time quantitative PCR (qPCR). Primers for the interest genes *nosZ* and *nirK* were designed by Yoon *et al.* (2015), and primers for reference genes *rpoB* and *recA* (Rocha, Santos and Pacheco, 2015) were designed in this study, using Primer-BLAST (Ye *et al.*, 2012). A list of the chosen primer sets for PCR and qPCR reactions are displayed in Table 1.

Samples taken for RNA extraction were immediately centrifuged at 4ºC and 5000 g for 10 minutes, for cells precipitation from culture media. The supernatant was discarded, and the pellet washed with 10 mL PBS 1x. The tubes were centrifuged again in the same conditions, and the supernatant discarded. The cells pellet was flash frozen in liquid nitrogen and stored at -80ºC until RNA extraction. The tubes used in this cell precipitation and washing method were kept on ice, whenever possible.

Table 1: Primers used in PCR and qPCR protocols to target *nosZ, nirK, rpoB, and recA*.

Gene	Reference	Product length (bp)	Primer	Sequence (5'→3')	Primer length (bp)	Tm (ºC)	%GC content
nosZ	(Yoon *et al.*, 2015)	160	SlonosZ599f	ATGGTAAGGAGACGCTGGAA	20	58,4	50,0
			SlonosZ758r	TTGTAGCAGGTAGAGGCGAAG	21	59,5	52,4
nirK	(Yoon *et al.*, 2015)	188	SlonirK853f	AAGGTGGGTGAGTCTGTGCT	20	61,1	55,0
			SlonirK1040r	GGCTGGCGGAAGGTGTAT	18	59,4	51,1
rpoB	This work	123	SlrpoB2538f	GGGTAGCGAAGAGATCACCG	20	60,0	60,0
			SlrpoB2660r	TTACCAACCAGGATGTCGCC	20	60,0	55,0
recA	This work	117	SlrecA725f	AGACTCGCGTTAAGGTGGTG	20	60,0	55,0
			SlrecA841r	TCACGCCAAGGTCTACCAAC	20	60,0	55,0

RNA extraction was performed with RNeasy Plus Mini Kit by Qiagen, following manufacturer's protocol. For the final step of the protocol, two elutions of RNA were performed, with 40 µL each. Afterwards, RNA from both elutions was quantified by nanodrop in DeNovix DS-11 FX. RNA elutions with best reading values of A260/A230 and A260/A280 proceeded to the next steps.

Furthermore, RNA samples were purified from any genomic DNA that could be present. This was done following the protocol from Thermo Scientific RapidOut DNA Removal Kit by Thermo Scientific. To verify RNA purity, *i.e.* no DNA contamination, a PCR reaction was prepared targeting the gene *recA* to confirm no amplification. Primers were SlrecA725f and SlrecA841r (Table 1). For a final volume of 25 µL, the mix was: PowerUp SYBR Green Master Mix from appliedbiosystems by Thermo Fisher Scientific (12,5 µL), forward primer (1,25 µL), reverse primer (1,25 µL), nuclease free H2O (8 µL), template (2 µL). A positive control was added, using *S. loihica* PV-4 previously extracted DNA, and a negative control was also prepared. In this assessment of RNA purity, we used RNA from before and after the purification described before. PCR reaction was: 50ºC 2 min.; 95ºC 5 min.; 35 cycles of 95ºC 15 sec., 55ºC 30 sec., and 72ºC 15 sec.; 72ºC 7 min; and a final stage of 4ºC for indefinite time. PCR products were run in 1,5% Agarose gel in TAE 1X at 140V for 35 minutes. Contrarily to non-treated RNA, no amplification was observed in the treated RNA, confirming the absence of DNA contamination. Agarose gel photographs taken with Bio-Rad Gel Doc XR+ showing these results are in Appendix A.

cDNA was synthetized from treated RNA for qPCR, using QuantiNovaTM Reverse Transcription Kit by Qiagen. The amount of treated RNA used for cDNA synthesis from each sample was 114 ng. Resultant cDNA was stored at -20ºC until further use.

Gene standards of *nosZ*, *nirK*, *recA*, and *rpoB* for qPCR were prepared by PCR of extracted DNA from a colony of *S. loihica* PV-4 growing in Luria-Bertani Agar. In the preparation of every qPCR reaction, fresh standard dilutions were prepared, accounting for 8 standards in total for every qPCR reaction, ranging from 10^2 to 10^9 copies/µL. For a final volume of 20 µL, the mix for real-time qPCR was: PowerUp SYBR Green Master Mix from appliedbiosystems by Thermo Fisher Scientific (10 µL), forward primer (1 µL, for a final concentration of 0,5µM), reverse primer (1 µL, for a final concentration of 0,5µM), nuclease free H2O (7 µL), template cDNA (1 µL). Optimization of the annealing/elongation step of qPCR was also performed, resulting in a best result of 60ºC for *nosZ*, 58ºC for *nirK*, 60ºC for *recA*, and 59ºC for *rpoB*. The reaction of qPCR had a 95ºC denaturation step (15s) followed by 58, 59 or 60ºC annealing/elongation step (60s), for 40 cycles, and a melting curve in the end. Relative expression of the interest genes *nosZ* (1) and *nirK* (2) was calculated by relating their quantified expression by qPCR with the quantified expression of the reference genes *recA* and *rpoB*, following the equations:

$$\textit{nosZ} \text{ relative expression} = \frac{\textit{nosZ} \text{ copies/well}}{\frac{\textit{recA} \text{ copies/well} + \textit{rpoB} \text{ copies/well}}{2}} \quad (1)$$

$$\textit{nirK} \text{ relative expression} = \frac{\textit{nirK} \text{ copies/well}}{\frac{\textit{recA} \text{ copies/well} + \textit{rpoB} \text{ copies/well}}{2}} \quad (2)$$

Physicochemical Parameters

In the Bio-Xplorer 400P system there is a continuous monitoring of pH, dissolved oxygen (DO), temperature, pressure, and air mass flow for each individual bioreactor. Data are monitored in real-time and stored every 20 seconds.

After all experiments, we retrieved the data for pH and temperature from each bioreactor. It would be interesting to reveal and analyze the variations of DO throughout the experiments. However, the stored DO data could not be retrieved due to a software error. Still, DO was monitored in real-time and was an important feature of our experimental design since it allowed us to determine the anoxic conditions and initiate gas and liquid sample collection

Statistical analysis

All statistical analysis were performed with IBM SPSS Statistics software (IBM Corp., 2021). We began by assuring the normality of our data. The data for N_2O flux in the cadmium treatment do not follow normality since all results are zero. However, and being aware that the t-test might have deviations, we will analyze them as well.

Gas samples from one reactor of the mid-exponential experiment were lost during N_2O measurements in GC-ECD. So, for statistical analysis of the effect of the treatment on the N_2O flux we have a number of cases of n=7 (3 cadmium, 4 control). For statistical analysis of the effect of the treatment on the relative expression of *nirK* and *nosZ*, we only considered the sampling points during the anoxic period, achieving a number of cases of n=6 (3 cadmium, 3 control) for each gene.

To assess the significance of the effect of the treatment, cadmium or control, on the N_2O flux, and *nirK* and *nosZ* relative expressions, we run a t-test for independent samples for each variable, with a significance of 5% (p-value = 0,05). At the same time, homoscedasticity was assessed by Levene's test.

Statistical analysis was only performed for the mid-exponential experiment due to the lack of replicates for the late-exponential experiment.

Outputs of the tests are displayed in Appendix B.

Results and Discussion

Selection of the deep-sea isolates

With the results from the IMG database search, we constructed a graphic to show bacterial class diversity after applying every filter to the search.

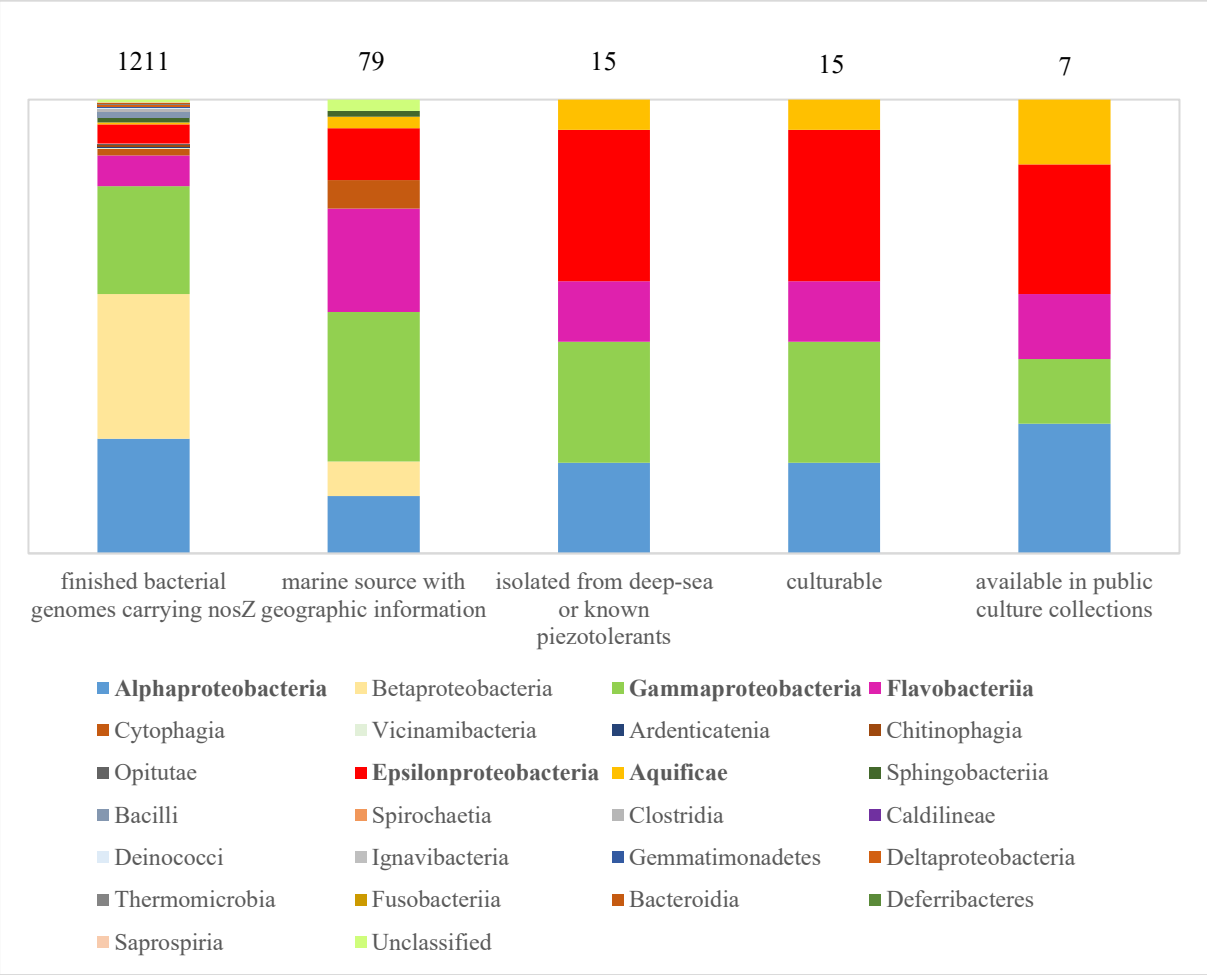

Figure 4: Graphical representation of bacterial class diversity through application of sequential search filters for the selection of four deep-sea isolates to work with. Applied search filters: bacteria with finished genomes carrying the *nosZ* gene → marine source isolates with geographic information → isolates from deep-sea or known piezotolerants → culturable isolates → isolates available in public culture collections. Above every bar there is the number of strains found in that search. The five classes represented in the last search, and last bar, are in bold (Alphaproteobacteria, Aquificae, Epsilonproteobacteria, Flavobacteriia, Gammaproteobacteria).

Bacterial class diversity lowers by the application of any filter, with the exception of the search for culturable strains. However, only 1211 finished bacterial genomes carrying *nosZ* is a very low number, considering all the 100303 finished, draft and permanent draft genomes in this

database (Chen *et al.*, 2021). This illustrates the lack of knowledge and public data on denitrifying bacteria, especially in the deep-sea, and urges us to fill the gaps.

The seven strains that persisted after all search filters (last column of Figure 4) are displayed in Table 2.

Most of the *nosZ* clades from those strains are not described in literature, so we constructed a phylogenetic tree relating NosZ protein sequences of 45 strains, displayed in Figure 2, to unveil that information.

Table 2: Isolates found after search in DOE Joint Genome Institute – IMG database, matching the criteria: bacteria with finished genomes carrying the *nosZ* gene; marine source isolates with geographic information; isolates from deep-sea or known piezotolerants; culturable isolates; isolates available in public culture collections.

Strain	**Phylum**	**Class**	**Genome ID**	***nosZ* clade**
Lutibacter profundi LP1	Bacteroidetes	Flavobacteriia	2663763042	Clade II
Nitratifractor salsuginis E9I37-1	Proteobacteria	Epsilonproteobacteria	649633076	Clade II
Persephonella marina EX-H1	Aquificae	Aquificae	643692030	Clade II
Profundibacter amoris BAR1	Proteobacteria	Alphaproteobacteria	2898017394	Clade II
Shewanella loihica PV-4	Proteobacteria	Gammaproteobacteria	2521172611	Clade I
Sulfurimonas autotrophica OK10	Proteobacteria	Epsilonproteobacteria	648028058	Clade II
Thalassospira indica PB8B	Proteobacteria	Alphaproteobacteria	2840662270	Clade I

From those seven isolates matching all criteria, the four most likely to grow faster in the laboratory were selected: *Shewanella loihica* PV-4, *Thalassospira indica* PB8B, *Lutibacter profundi* LP1, and *Profundibacter amoris* BAR1.

Regarding the selected four strains for further work, *Shewanella loihica* PV-4, shown in Figure 3 (a), is a Gram-negative bacterium, belonging to the Gammaproteobacteria class, polarly flagellated, facultative anaerobic and psychrotolerant, with a growth temperature range from 0 to 42ºC, and pH range for growth of 4,5-10,0. The type strain was isolated from an iron-rich microbial mat in the deep-sea hydrothermal Naha Vent on the South Rift of Loihi Seamount, Hawaii, Pacific Ocean, 1325 meters below sea level (Gao *et al.*, 2006a). This strain belongs to clade I *nosZ* (Hallin *et al.*, 2018), and has functional pathways for denitrification and respiratory ammonification (Yoon, Sanford and Löffler, 2015).

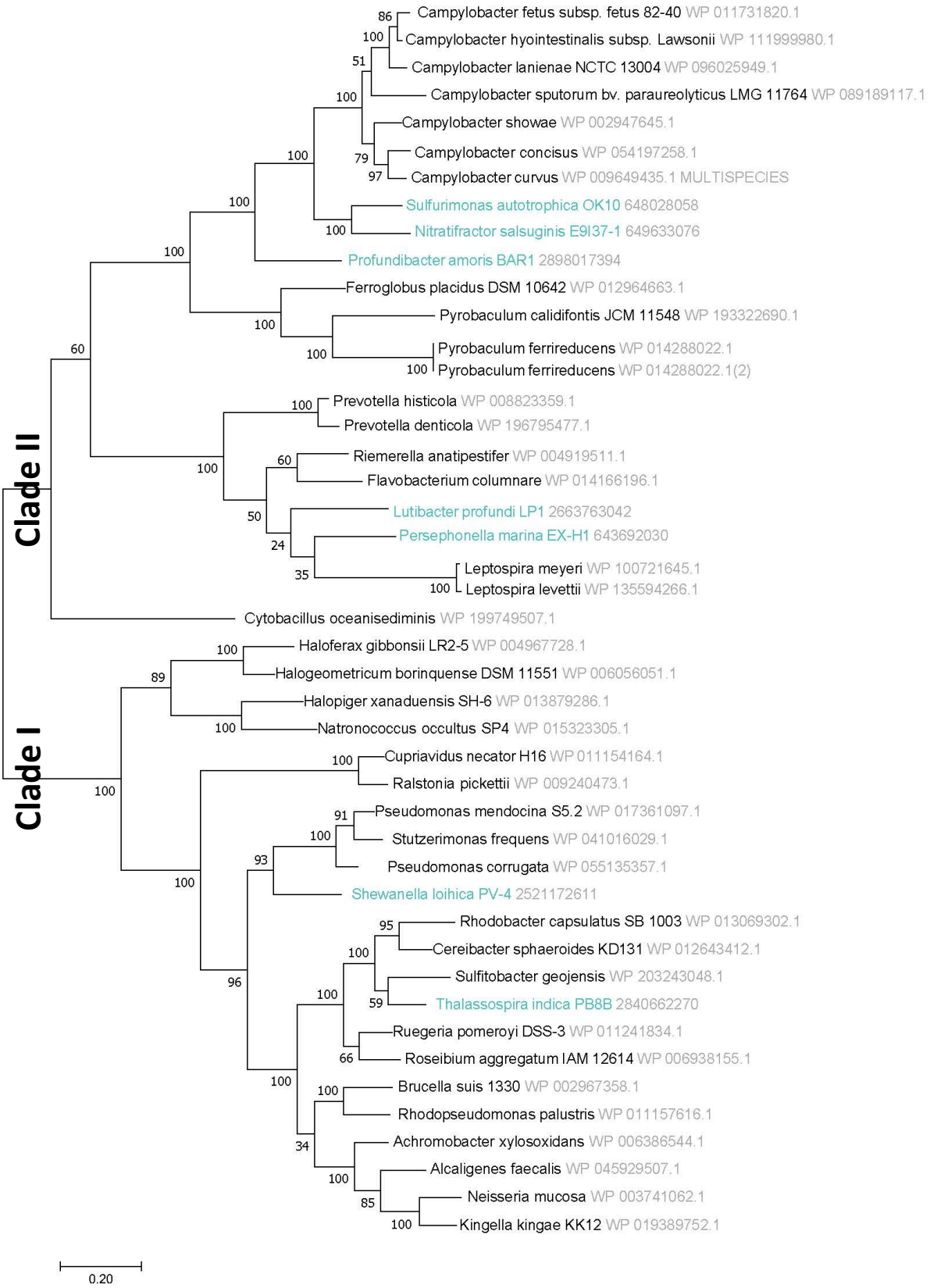

Figure 2: Maximum likelihood phylogeny of NosZ aminoacid sequences obtained from 45 sequences from different strains showing the grouping of clades I and II. Strains in blue are the seven referred in Table 2. In grey, are protein accession numbers retrieved from National Center for Biotechnology Information – NCBI, and in grey following in blue strains is the GenomeID from the IMG database.

Thalassospira indica PB8B, Figure 3 (b), is a Gram-negative bacterium, belonging to the class Alphaproteobacteria, with curved rods and motile cells, facultatively anaerobic, growth temperatures ranging from 10ºC to 41ºC, and pH range for growth of 5-11. The type strain was isolated from Indian Ocean (24° 31′ 12″ S 69° 55′ 34.32″ E) at a depth of 2200 meters (Yang Liu *et al.*, 2016). This strain belongs to clade I *nosZ* (Table 2).

Lutibacter profundi LP1 is a Gram-negative bacterium, belonging to the class Flavobacteriia, with rod-shaped cells under optimal conditions, non-motile, microaerophilic, a growth temperature range from 13 to 34ºC, and pH range for growth of 5,5-7,5. The type strain was isolated from a bacterial mat growing on a black smoker hydrothermal chimney within the Loki's Castle hydrothermal system (73°33′ N 08°09′ E), Atlantic Ocean, at a depth of 2350 meters (Bauer *et al.*, 2016). This strain belongs to clade II *nosZ* (Table 2). *L. profundi* LP1 is microaerophilic, meaning it requires low concentrations of oxygen to grow. Instructions for its cultivation included keeping the Marine Agar plates surface moist by adding Marine Broth regularly. For that reason, it is not possible to see individual bacterial colonies on plate, see Figure 3 (c).

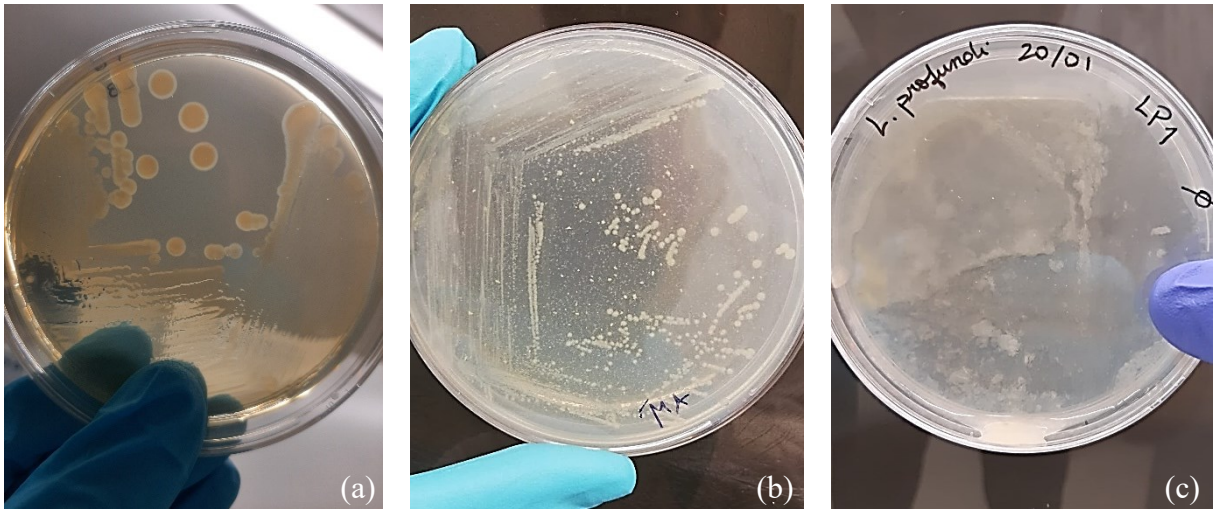

Figure 3: Photographs of the strains growing in plates: (a) *Shewanella loihica* PV-4, (b) *Thalassospira indica* PB8B, and (c) *Lutibacter profundi* LP1.

Profundibacter amoris BAR1 is a Gram-negative bacterium, belonging to the phylum Proteobacteria, with rod-shaped cells, some motile cells in young cultures, a growth temperature range from 10 to 37ºC, and pH range for growth of 5,5-8 (Bauer *et al.*, 2019). This strain is piezophilic and grows under anaerobic, microaerobic and aerobic conditions, and the type strain was isolated from a microbial mat growing on the surface of a barite chimney at the

Loki's Castle Vent Field, Arctic Mid-Ocean Ridge, at a depth of 2216 meters (Bauer *et al.*, 2019). This strain belongs to clade II *nosZ* (Table 2).

After activation of the acquired strains, it was noticed that *P. amoris* BAR1 didn't grow in the timeframe of seven weeks, so this strain was excluded for further experiments. Among the remaining three, besides having a more explored N_2O pathway, *S. loihica* PV-4 was the strain that grew faster, so we selected it for the core experiments of this thesis.

Growth with different cadmium concentrations

Shewanella loihica PV-4 and *Thalassospira indica* PB8B grew with $CdCl_2$ concentrations of 0,01 and 0,025 mM, while *Ruegeria pomeroyi* DSS-3 only grew with 0,01 mM achieving half the growth compared to its control (no cadmium). In Figure 5, we can see the growth curves from this experiment.

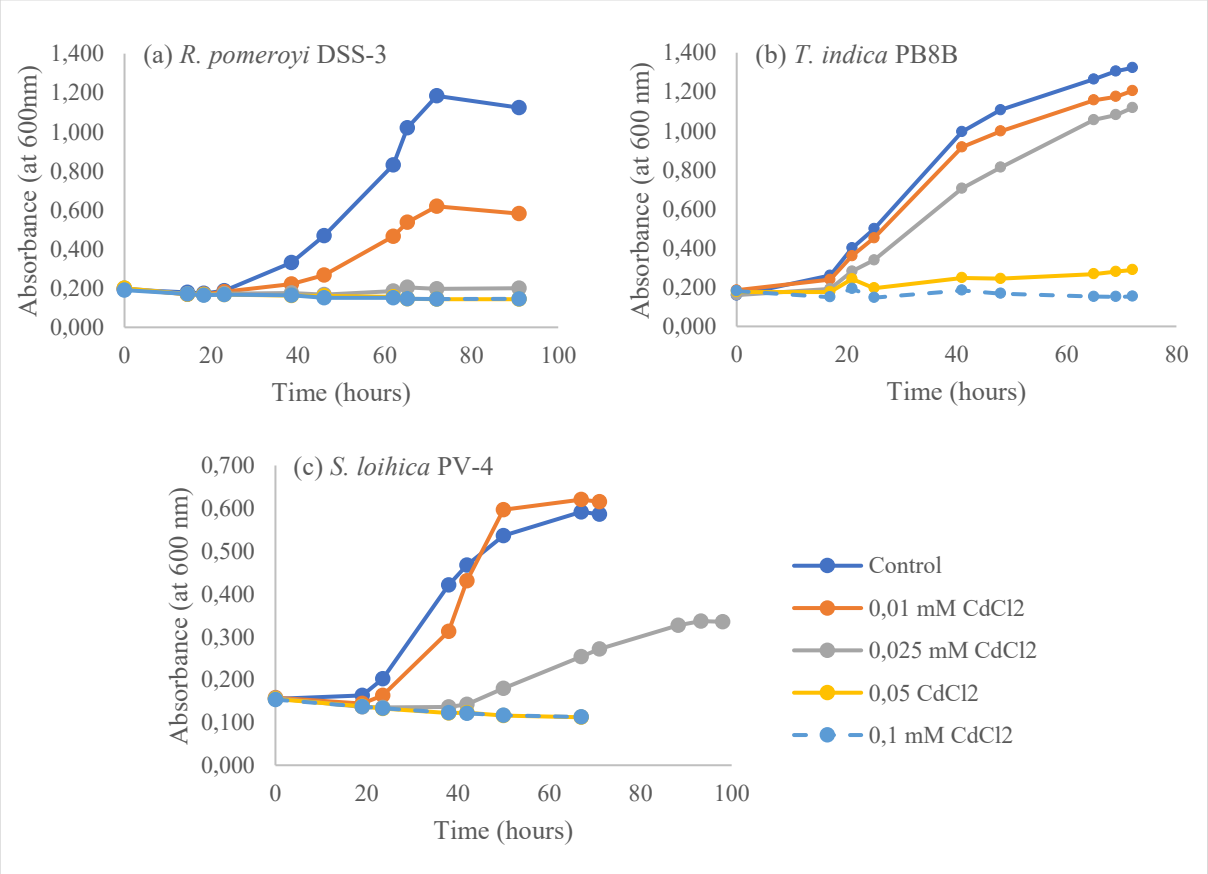

Figure 5: Growth graphics with four different $CdCl_2$ concentrations and control for (a) *Ruegeria pomeroyi* DSS-3, (b) *Thalassospira indica* PB8B, and (c) *Shewanella loihica* PV-4.

For the same concentration of $CdCl_2$ in solution, 0,01 mM, *S. loihica* PV-4 and *T. indica* PB8B grow similarly to their control without cadmium, and *R. pomeroyi* DSS-3 growth is

approximately half when compared to its control. Because 0,01 mM $CdCl_2$ appears to not affect *S. loihica* PV-4 growth, when compared to control, we chose this concentration for further experiments with this strain.

It is worth noticing that *S. loihica* PV-4 and *T. indica* PB8B were able to grow with 0,025 mM $CdCl_2$, a concentration that appears to inhibit *R. pomeroyi* DSS-3 growth. This result suggests that the two deep-sea strains, *S. loihica* PV-4 and *T. indica* PB8B, are less sensitive to cadmium than *R. pomeroyi* DSS-3, a pelagic strain. This can be linked to cadmium distribution in the oceans. Cadmium concentrations are known to be lower in surface waters and to increase with depth (J. *et al.*, 2014)(Xu and Morel, 2013), so we believe that, since *S. loihica* PV-4 and *T. indica* PB8B were isolated from the deep-sea, they might be less sensitive to this metal than a pelagic strain. Adaptation to deep-sea environmental conditions may affect sensitivity to potential stressors (Brown *et al.*, 2017), such as metals, although deep-sea vs pelagic bacteria sensitivity to metals is still poorly understood. In fact, it is challenging to compare deep-sea and pelagic bacteria sensitivity to metals only by culture-dependent methods once temperature, oxygen concentration, and hydrostatic pressure together have impact on toxic metals sensitivity (Brown, Thatje and Hauton, 2017).

Core experiments with Shewanella loihica *PV-4 and N_2O metabolism investigation*

Growth during experiments

Growth of *Shewanella loihica* PV-4 during all experiments (A, B, and C – replicated experiments performed in different days) was measured and it is shown in Figure 6. It is clear to notice that the growth in the three experiments is not identical. Despite trying to minimize heterogeneity during the pre-experiment culture growth, we can see that the start of the exponential phase changes between experiments, being later in experiment A, and sooner in experiment C. Also, when comparing cadmium and control reactors within the same experiment, it appears that cadmium treatment delays the beginning of the exponential phase.

In these experiments, the aim was to induce an anoxic period in the mid-exponential phase, when we would also retrieve gas samples for N_2O measurements and biomass for RNA extraction. However, in the first experiment (experiment A) we could only perform the anoxic part of the experiment in the late-exponential phase of culture growth, as it is possible to recognize in Figure 6. For that reason, and because it has been shown that mid-exponential and late-exponential bacterial metabolism can be quite different (Chubukov *et al.*, 2014; Molina *et al.*, 2019) we grouped experiments B and C, and separated them from A.

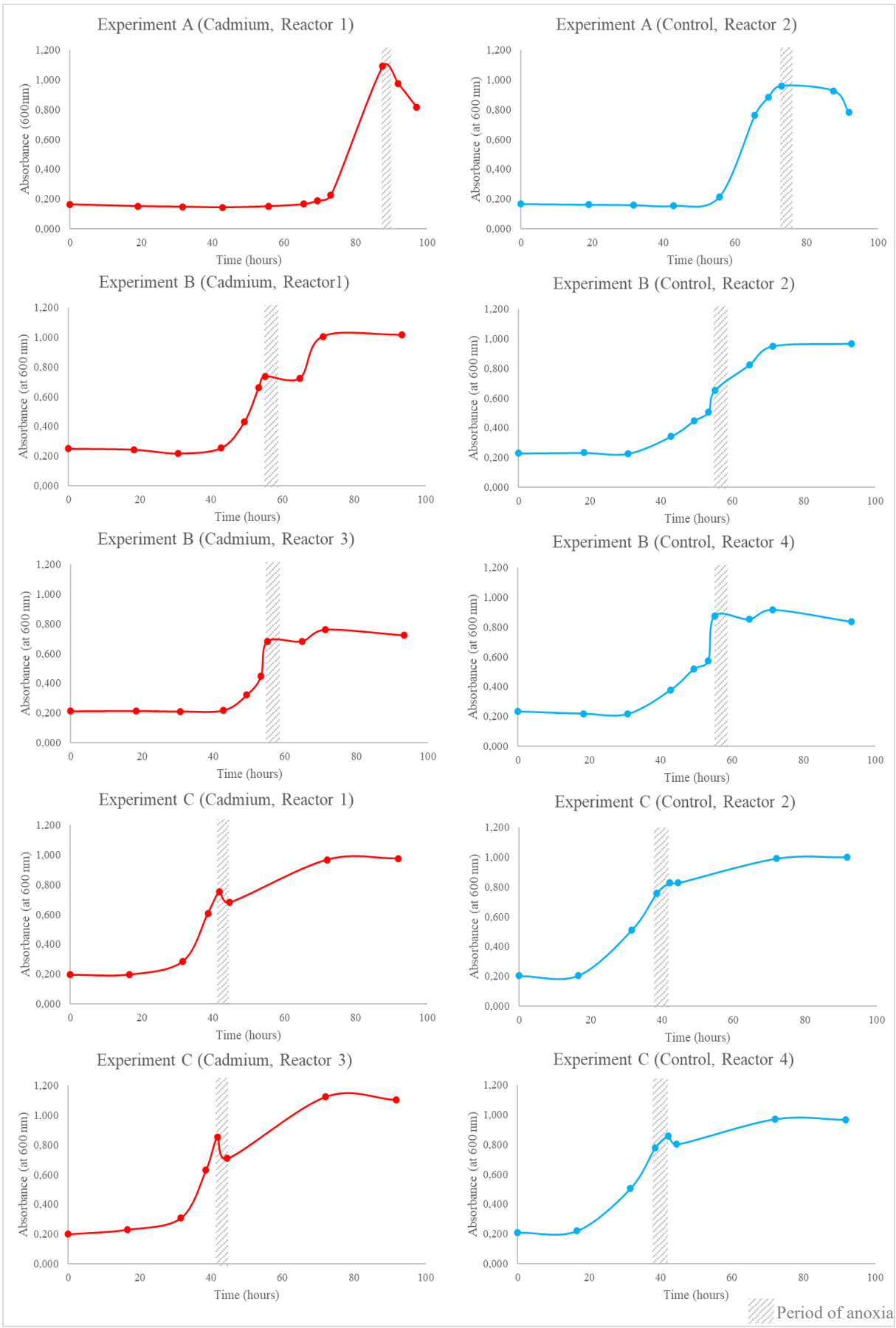

Figure 6: *S. loihica* PV-4 growth in each reactor from experiments A, B and C.

From now on, the results will be present referring to mid-exponential experiment (B and C), and late-exponential experiment (A). This brings a problem regarding experimental replication, as the late-exponential experiment only has 1 replicate for each treatment. Nevertheless, and being aware of the possible misrepresentation of the results, late-exponential experiment results will be presented and discussed as they can provide novel information.

Physicochemical conditions

The graphical data regarding pH and temperature inside the reactors, retrieved from the software associated to Bio-Xplorer 400P, is displayed in Figures 7 to 16.

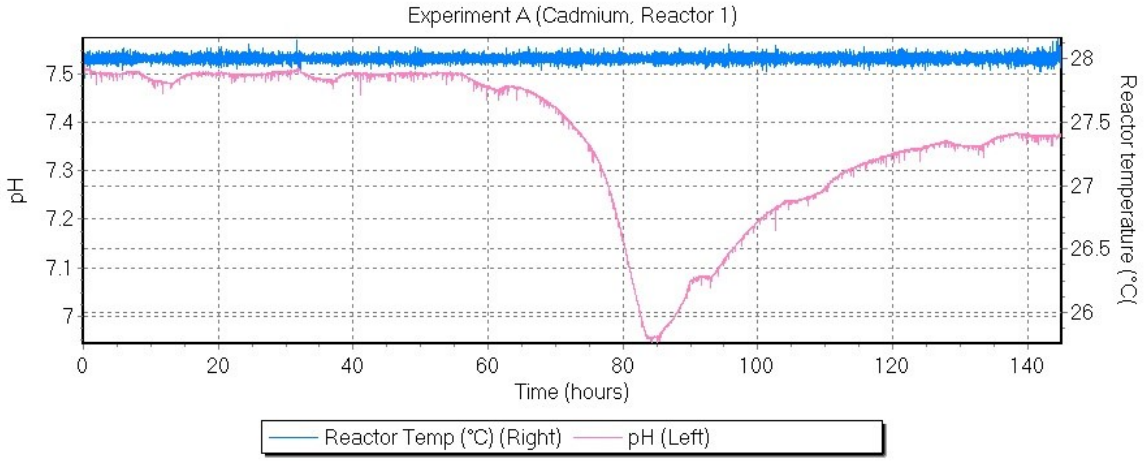

Figure 7: Reactor temperature and pH from reactor 1, cadmium treatment, during the late-exponential experiment.

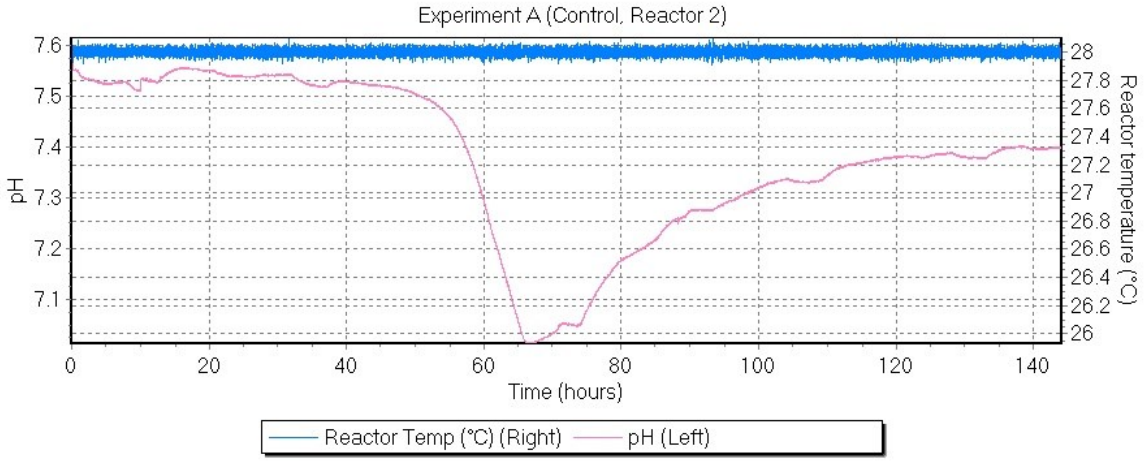

Figure 8: Reactor temperature and pH from reactor 2, control treatment, during the late-exponential experiment.

In the late-exponential experiment, Figures 7 and 8, the reactor temperature remains constant throughout the experiment. However, the pH has a drop from ≈7,5 to ≈7 which corresponds to approaching the late phase of exponential growth and the period where there is no more O_2

supplying. Numerous variables can cause variations in the extracellular pH, such as the original pH and medium composition, the growth phase, and the physiology and ideal pH of the bacterium (Sánchez-Clemente *et al.*, 2018). *S. loihica* PV-4 is able to produce acid from N-acetyl-D-glucosamine, a derivative of glucose (Gao *et al.*, 2006b). It is a possibility that *S. loihica* PV-4 produces this when approaching the end of the exponential phase and acidifies the medium, but not enough to inactive its own growth because it continues to grow. In fact, *S. loihica* PV-4 appears to restore the pH to values that are close to initial.

This drop of pH is earlier in reactor 2 (Figure 8) than in reactor 1 (Figure 7), which is expected once, in this experiment, the control (reactor 2) reached the late-exponential phase of growth (considered time point = 73 hours) before the culture treated with cadmium (considered time point = 87,5 hours).

The temperature inside the reactors remained constant at 28ºC has expected.

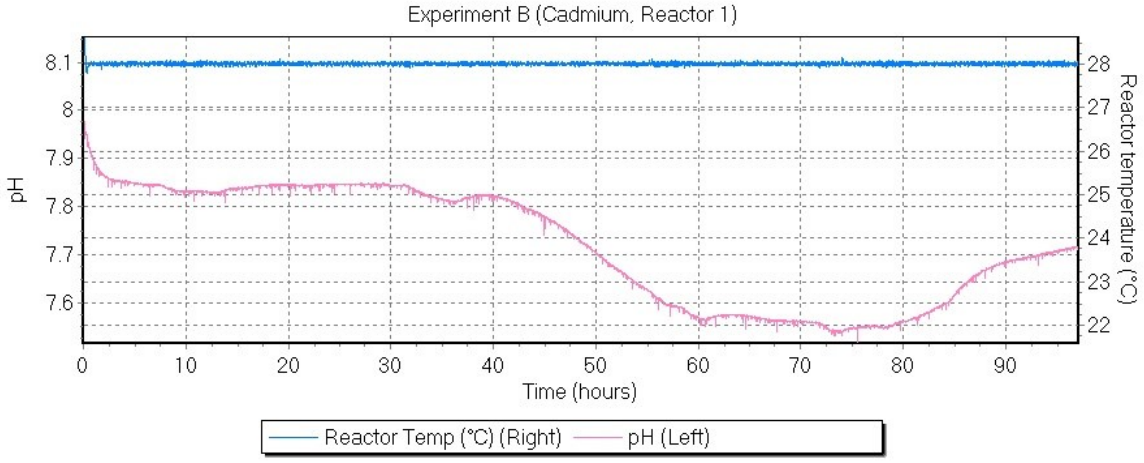

Figure 9: Reactor temperature and pH from reactor 1, cadmium treatment, of experiment B from the mid-exponential experiment.

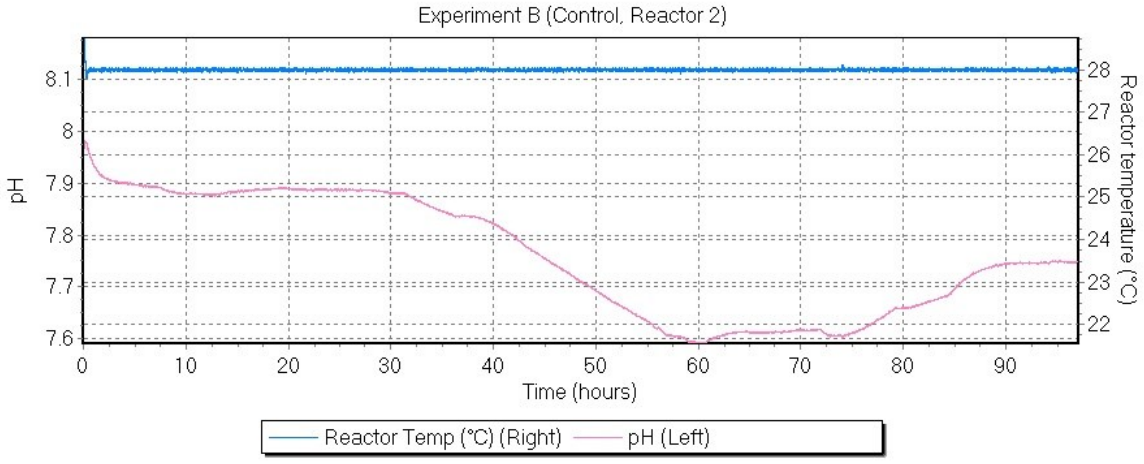

Figure 10: Reactor temperature and pH from reactor 2, control treatment, of experiment B from the mid-exponential experiment.

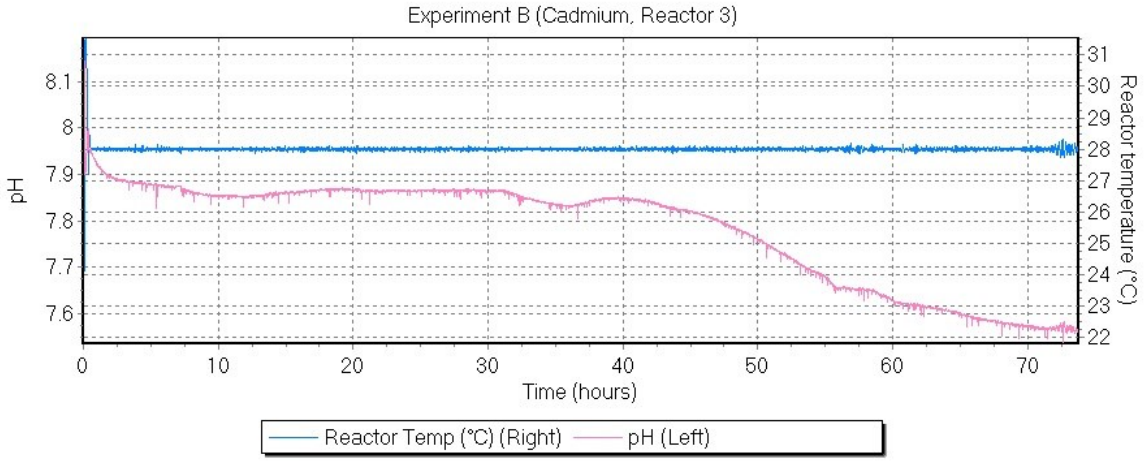

Figure 11: Reactor temperature and pH from reactor 3, cadmium treatment, of experiment B from the mid-exponential experiment.

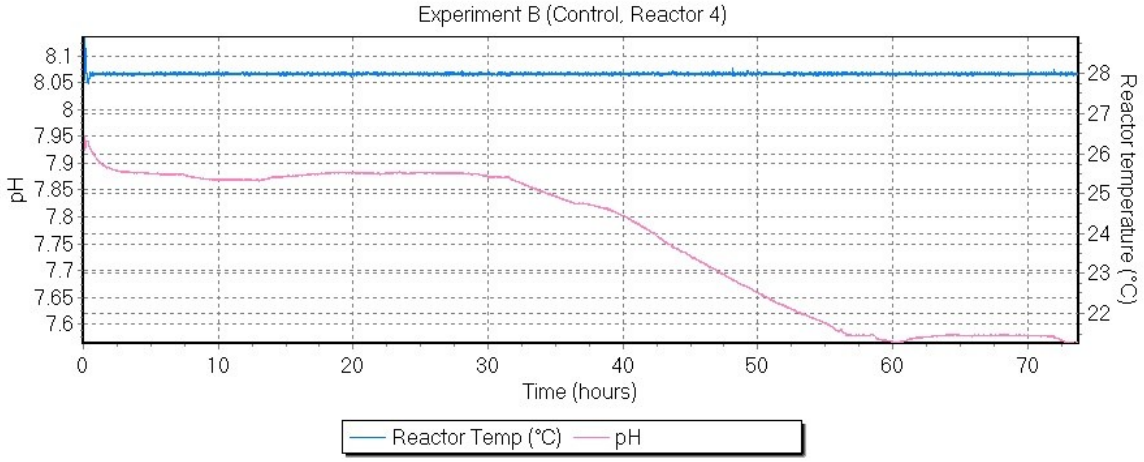

Figure 12: Reactor temperature and pH from reactor 4, control treatment, of experiment B from the mid-exponential experiment.

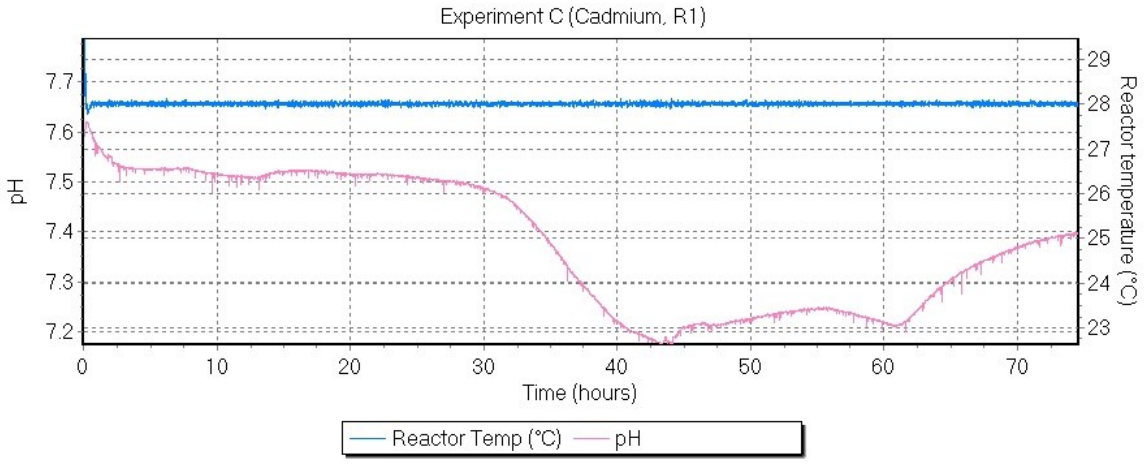

Figure 13: Reactor temperature and pH from reactor 1, cadmium treatment, of experiment C from the mid-exponential experiment.

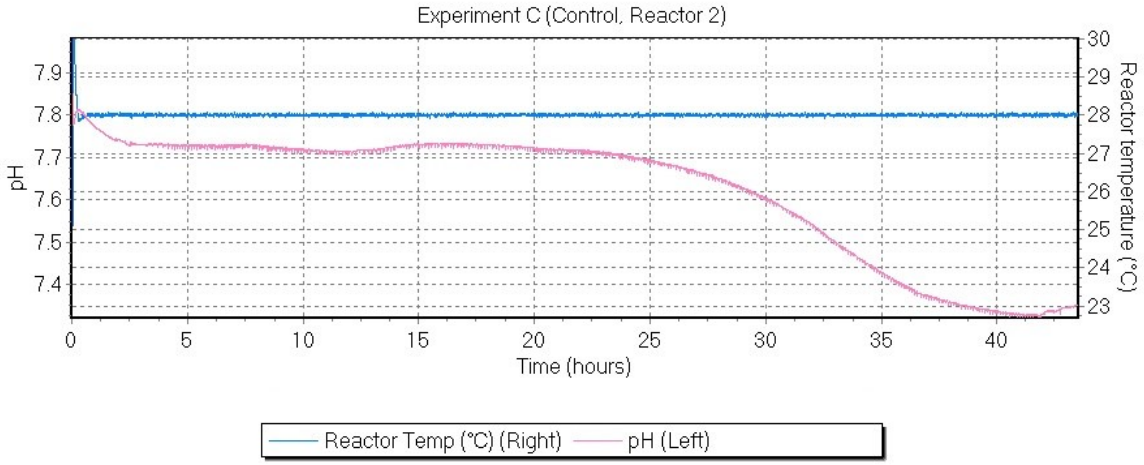

Figure 14: Reactor temperature and pH from reactor 2, control treatment, of experiment C from the mid-exponential experiment. *Note: experiment did not end at ≈45 hours, part of the results were lost.*

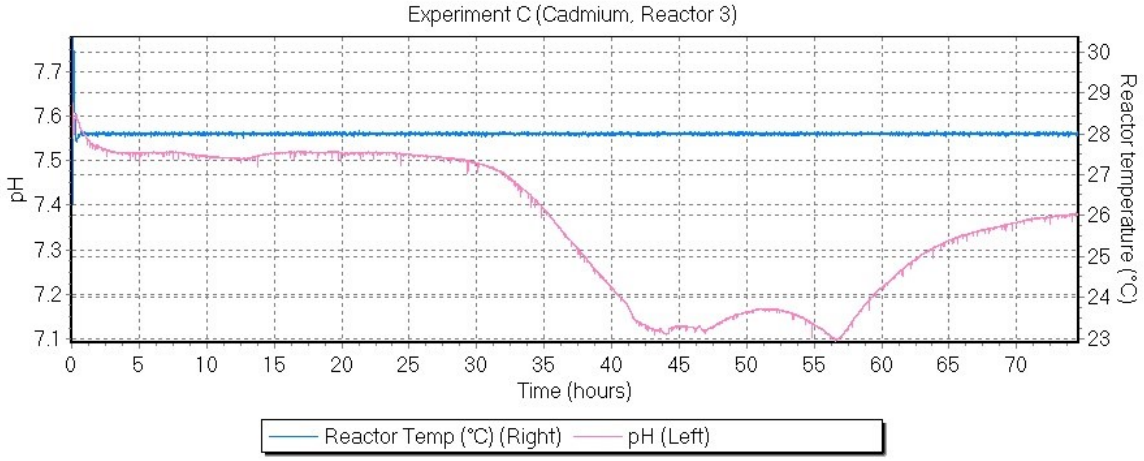

Figure 15: Reactor temperature and pH from reactor 3, cadmium treatment, of experiment C from the mid-exponential experiment.

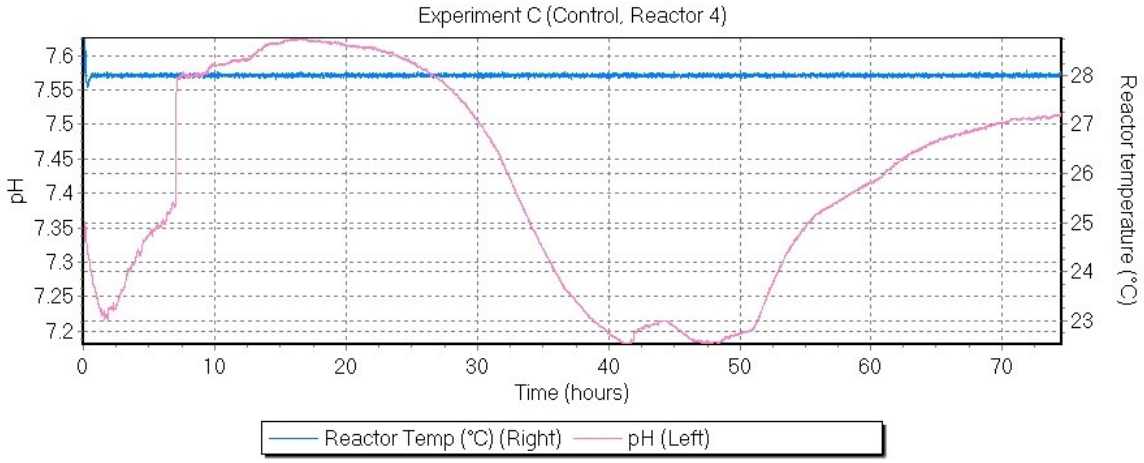

Figure 16: Reactor temperature and pH from reactor 4, control treatment, of experiment C from the mid-exponential experiment.

In the experiments B and C (Figures 9 to 16), that correspond to the mid-exponential experiment, the period of lower pH appears to be longer than in the reactors from the late-exponential phase (Figures 7 and 8). In the late-exponential experiment, the period of anoxia was induced after the lowest value of read pH. However, in the mid-exponential experiment the period of anoxia was induced during the decreasing of pH (time point of induced anoxia in all reactor from B = 55 hours; time point of induced anoxia in reactors 2 and 4 from C = 38,5 hours; time point of induced anoxia in reactors 1 and 3 from C = 41,75 hours).

By changing the growing conditions, bacteria can redirectionate their metabolism since their physiology is coordinated with their nutritional environment (Nguyen *et al.*, 2021). In fact, our experiment relies on that, since we induce a period of anoxia so that *Shewanella loihica* PV-4 is able to produce and reduce N_2O.

pH homeostasis is the regulation of the pH both inside and outside of the cell and it has a significant impact on the uptake and use of nutrients, the breakdown of substrates, and the production of proteins and nucleic acids, making it essential for cell development and metabolism (Guan and Liu, 2020)

Possibly, by changing the growing conditions in a highly active metabolic phase of growth (mid-exponential), the culture directionated their metabolism towards adapting to that new environment rather than restoring the pH, due to the fact that neutral internal pH requires a lot of energy to maintain, which significantly limits microbial growth and metabolism.

Cadmium quantification

Graphics containing the standards curves and respective linear regressions are displayed in Appendix C. Parting from the linear regressions, we calculated the cadmium concentration in each sample. Results are displayed below in Table 3.

Initial samples (Table 3, “Beginning of experiment”) were taken right after the inoculation of the media in reactors, and the final samples (Table 3, “End of experiment”) were taken after stabilization of the stationary phase of bacterial growth, right before ending the experiment and disassembling the reactors.

Expected cadmium (Cd) concentration in initial samples is 1,83 mg/L (MM Cd = 183,32 g/mol, target $[Cd]_{\text{in solution}} = 0{,}01$ mM). Slightly lower cadmium concentrations in initial samples might be due to accumulated experimental errors, such as scaling and volume adjusting in the media composition, addition of glucose and nitrate and/or the addition of the $CdCl_2$ solution itself.

Cadmium ions (Cd^{2+}) can become adsorbed on the bacterial cells (Mullen *et al.*, 1989). Between initial and final samples there is a high increase in bacterial cells, so the possible adsorption of

cadmium to cells, linked to bacterial growth throughout the experiment, can be a cause for cadmium concentrations dropping from initial to final samples.

Table 3: Cadmium concentrations in samples from begging and end of the experiment, for each reactor, for each experiment. Mean and standard error of cadmium concentrations are displayed per treatment for mid-exponential and late-exponential experiments. Letters indications refers to the experiment (A, B or C) and the numbers (1, 2, 3 and 4) refer to the reactor.

			Cadmium concentration (mg/L)			
Experiment	**Treatment**	**Replicate**	Beginning of experiment	**Mean ± SEM**	End of experiment	**Mean ± SEM**
Mid-exponential	Cadmium	B1	1,65	**1,67 ± 0,06**	0,69	**0,69 ± 0,05**
		B3	1,85		0,54	
		C1	1,63		0,77	
		C3	1,55		0,75	
	Control	B2	< 0,05	**< 0,05**	< 0,05	**< 0,05**
		B4	< 0,05		< 0,05	
		C2	< 0,0125		< 0,0125	
		C4	< 0,0125		< 0,0125	
Late-exponential	Cadmium	A1	1,29	**1,29**	0,80	**0,80**
	Control	A2	< 0,05	**< 0,05**	< 0,05	**< 0,05**

Metal adsorptions are dynamic, since there is an equilibrium between the available Cd^{2+} and binding sites on cells, or even binding to other compounds in solution.

Furthermore, we should consider the possibility of mechanisms other than surface adsorption when working with bacterial cells. Other processes can include cadmium precipitation on cell surface and active absorption by nonspecific cation transport systems (Mullen *et al.*, 1989).

Further experiments would have to be performed to understand if cadmium is being actively uptake by *S. loihica* PV-4 in these experiments, if it is only being adsorbed on cells, complexed with other compounds present in the media, or precipitating.

Cadmium effect on net N_2O production

Reactor headspace samples taken overtime after anoxia were measured for N_2O quantification and assessment of net N_2O production. As net N_2O production derives from consumption and production rates, we determined the N_2O flux for each treatment in the mid-exponential and late-exponential experiments. Figure 17 presents the results of the N_2O quantification in headspace samples taken over time, and the calculated N_2O fluxes.

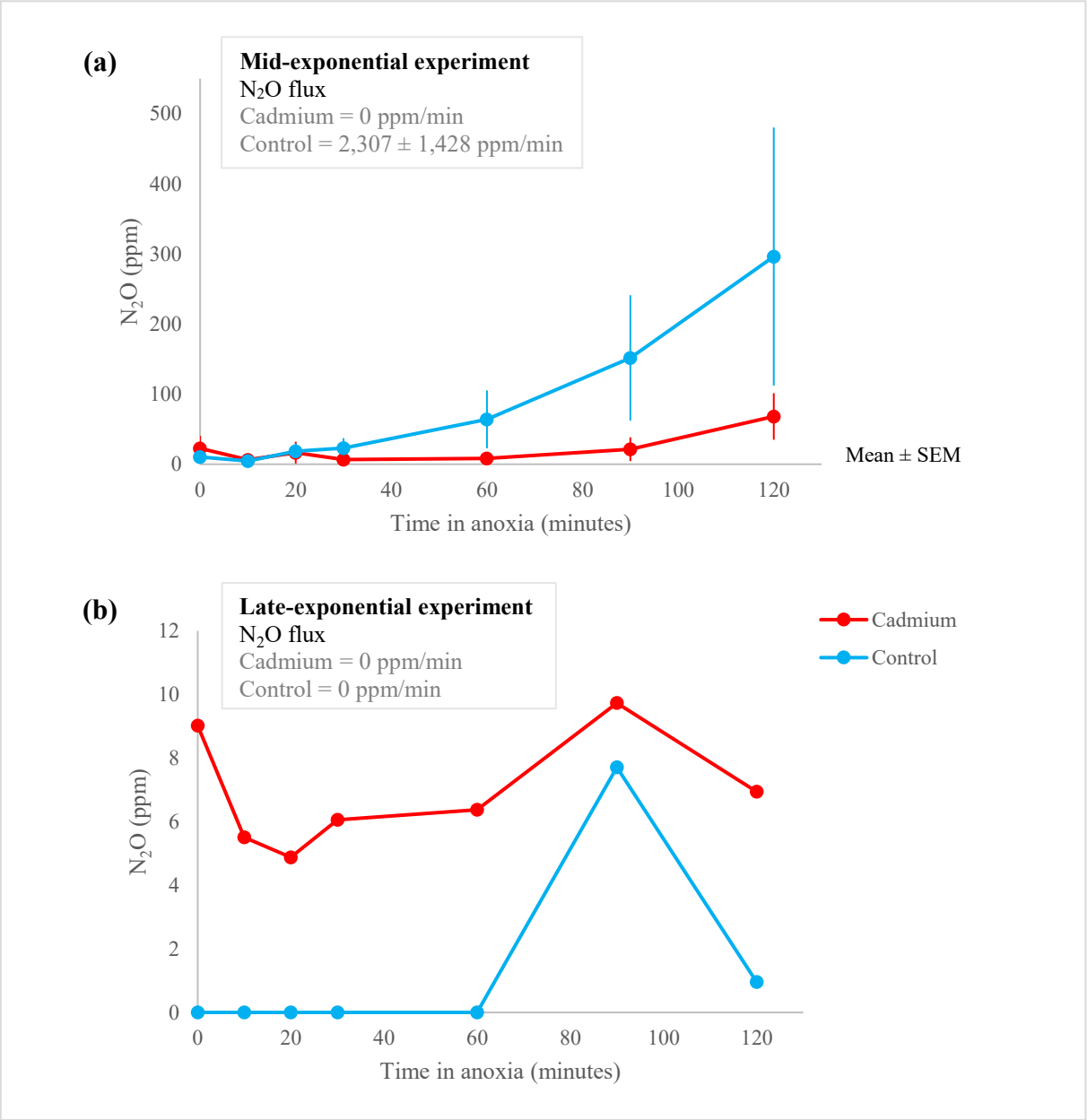

Figure 17: Quantified N_2O in gas samples taken over time after anoxia, and the calculated N_2O fluxes for each treatment, cadmium and control, in the (a) mid-exponential experiment and (b) late exponential experiment.

In the mid-exponential experiment, *S. loihica* PV-4 treated with cadmium seem to have different response patterns than in control (independent samples t-test, $p<0,05$, cadmium variable does not follow normal distribution), and inverse patterns that the ones seen in late-exponential experiment.

Control N_2O shows a positive flux in the mid-exponential experiment (Figure 17 a), comparing to a null flux in the late-exponential experiment (Figure 17 b). This might be due to the low or depleted carbon and electron source in the late-exponential phase of growth. With no glucose

left to oxidize, *S. loihica* PV-4 seems to have no capacity of producing or reducing great amounts of N_2O.

Notwithstanding the null fluxes observed in the late-exponential experiment in both treatments, the amount of background N_2O in cadmium treatment is significantly higher than in control. In this experiment (Figure 17 b), five control time points showed N_2O read values of 0 ppm (below detection limit) in contrast to the positive N_2O values registered for the cadmium treatment. Moreover, the cadmium treatment presented higher N_2O values than the control treatment across all timepoints.

It is important to say that there is a small time period, about 45 minutes, between changing the air flow from O_2 to N_2 and sampling the first time point of the anoxic part of the experiment. When the air flow is changed, there is a waiting time where the dissolved oxygen in media decreases slowly until it becomes close to zero. Possibly, in this period of decreasing oxygen, *S. loihica* PV-4 had a net N_2O production with higher production than consumption in the cadmium treatment and late-exponential experiment, explaining the presence of N_2O in the first time point of headspace sampling. Nevertheless, we should keep in mind that this experiment only has one replicate per treatment, and this behavior needs further confirmation.

In Table 4, we present the calculated slopes and R^2 for each reactor. Slopes for $R^2<0,80$ were only considered zero *a posteriori*.

Five gas samples from C1 were lost, remaining only two. The R^2 of that would be 1, and the slope could be misrepresentative, for that reason the results of that reactor were excluded from these calculations.

Table 4: Calculated slopes and R^2 for each reactor in mid-exponential and late-exponential experiments for further determination of N_2O fluxes. Letters indications refers to the experiment (A, B or C) and the numbers (1, 2, 3 and 4) refer to the reactor.

	Mid-exponential experiment								**Late-exponential experiment**	
	Cadmium				Control				Cadmium	Control
	B1	B3	C1	C3	B2	B4	C2	C4	A1	A2
Slope	0,766	0,062	-	0,207	-0,070	0,576	6,327	2,328	0,012	0,034
R^2	0,52	0,62	-	0,19	0,09	0,83	0,90	0,94	0,08	0,27

Table 5 illustrates the calculated N_2O fluxes for each treatment, considering the results in Table 4 and fluxes of zero for $R^2<0,80$.

In mid-exponential experiment (Figure 17 a), the control reveals a positive N_2O flux of 2,307 ± 1,428 ppm/min (Table 5) significantly higher than in cadmium treatment (independent samples t-test, $p<0,05$), suggesting that cadmium might inhibit net N_2O production in this growth condition.

Table 5: N_2O flux for each reactor in mid-exponential and late-exponential experiments. Mean N2O flux is presented in association to the standard error. Letters indications refers to the experiment (A, B or C) and the numbers (1, 2, 3 and 4) refer to the reactor.

	Mid-exponential experiment									**Late-exponential experiment**	
	Cadmium				Control					Cadmium	Control
	B1	B3	C3	Mean	B2	B4	C2	C4	Mean	A1	A2
N_2O flux (ppm/min)	0	0	0	0	0	0,576	6,327	2,328	2,307 ±1,428	0	0

Studies differ on results of cadmium effect on denitrification in aquatic habitats. Some relate increasing cadmium concentration with inhibition of denitrification (Sakadevan, Zheng and Bavor, 1999), while others say that cadmium enhances complete denitrification (Broman *et al.*, 2019). Magalhães *et al.* (2007) curiously suggests that cadmium, along with other trace metals, might have inhibitory effect on specific steps within the denitrification enzymatic system.

Cadmium effect on the relative expression of nirK *and* nosZ

To help unveiling the cellular mechanisms driving potential effects on net N_2O production, we studied the relative expression of the genes *nirK* and *nosZ*, that encode nitrite reductase and N_2O reductase, respectively, two essential enzymes in the denitrification process responsible for the reduction of NO_2^- to NO and N_2O to N_2, respectively.

Figures 18 and 19 represent the calculated *nirK* and *nosZ* relative expressions in the four samples taken over time. The first samples were taken in the moment right before turning the air flow in the reactors from O_2 to N_2. The time in the X axis marks the time since anoxia, so the time before anoxia is represented in the negative part of that same axis. Time = 0 marks the beginning of the anoxia period, where the dissolved oxygen in media is close to zero.

In mid-exponential experiment, both *nirK* and *nosZ* seem to have different response patterns between treatments, considering the time points in anoxia, although there is no significance found for that difference (independent samples t-test, p>0,05). Both relative expressions have higher values in control than in cadmium, and *nirK* relative expression is higher than *nosZ* relative expression for both treatments. To relate *nirK* to *nosZ*, the *nirK/nosZ* ratio was calculated.

For the mid-exponential experiment $nirK/nosZ_{CADMIUM}$ = 1,384 and $nirK/nosZ_{CONTROL}$ = 13,415. Both ratios are higher than 1, indicating a higher mean relative expression of *nirK* than *nosZ* in both treatments. The 10x higher *nirK/nosZ* ratio for control implies a much higher expression of *nirK* in this treatment, supporting the positive N_2O flux indicated in Figure 17 (a). Moreover, the low but higher than 1 value for $nirK/nosZ_{CADMIUM}$ indicates that, in these

conditions, the denitrification metabolic pathway is stronger in the direction of producing N_2O than in its reduction. This ratio not only supports the 0 ppm/min flux of N_2O calculated for this treatment, but also supports our immediate impression when looking at the N_2O quantity over time in the cadmium treatment, where it appears that N_2O is slowly increasing (Figure 17 a).

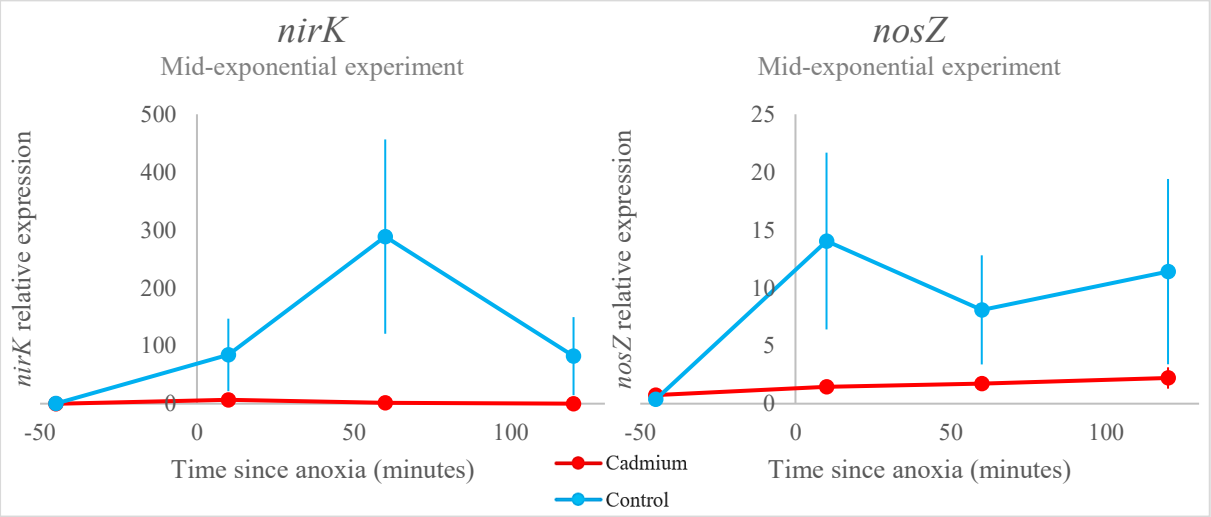

Figure 18: Graphs of *nirK* and *nosZ* relative expression over time in the mid-exponential experiment. Points represent Mean ± SEM.

In late-exponential experiment, expression responses of the target genes seem to be different between treatments. Contrary to the mid-exponential experiment, here both relative expressions have higher values in cadmium than in control, and *nosZ* relative expression is higher than *nirK* relative expression for both treatments.

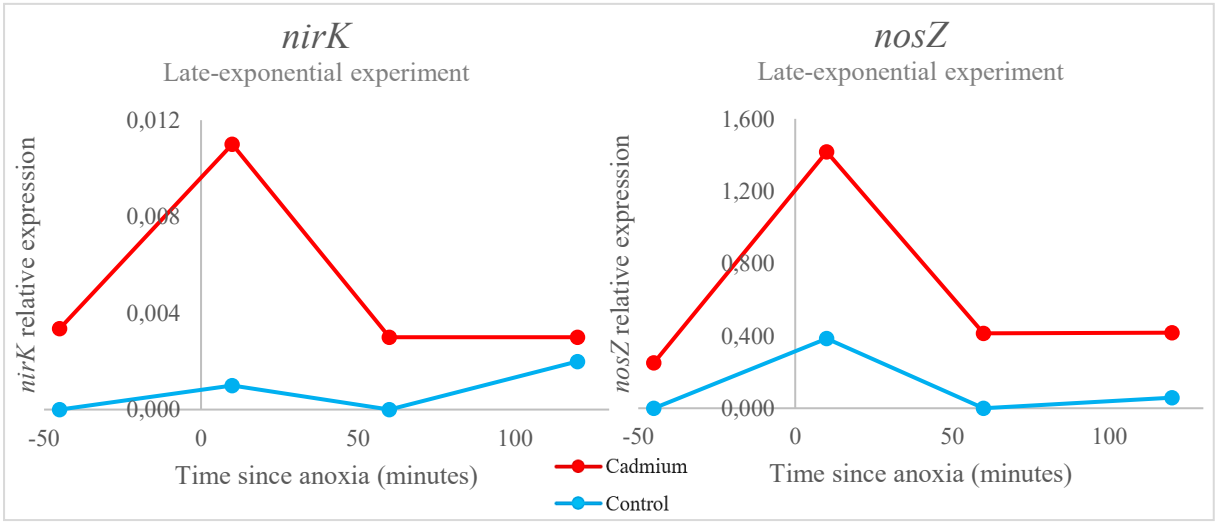

Figure 19: Graphs of *nirK* and *nosZ* relative expression over time in the late-exponential experiment.

For late-exponential experiment, $nirK/nosZ_{CADMIUM}$ = 0,008 and $nirK/nosZ_{CONTROL}$ = 0,007. Both are very low ratios, indicating a much higher mean relative expression of *nosZ* than *nirK*, that can explain the low values of quantified N_2O for both treatments of the late-exponential experiment, see Figure 17 (b), since much of the formed nitrous oxide could be reduced to N_2. Additionally, it is possible to see an abrupt decrease in genes relative expression in the cadmium treatment. In this treatment, although there is an initial increase in relative expression when the dissolved O_2 is dropping, between the first time point in anoxia (t = 10 min) and the last (t = 120 min) *nirK* has a decrease of 73%, and *nosZ* a decrease of 71%. These results support the N_2O quantification results displayed in Figure 17 (b), because with this low expression *S. loihica* PV-4 is not able to produce nor reduce N_2O, maintaining a relatively constant N_2O concentration in the headspace.

In the control treatment of the late-exponential experiment, between the first time point in anoxia (t = 10 min) and the last (t = 120 min), *nirK* presents an increase in relative expression of 100% and decrease of 85% in *nosZ* relative expression. *nirK* increase in relative expression can explain the N_2O peak, in control, observed at t = 90 min in Figure 17 (b).

Several studies state that cadmium decreases *nosZ* and *nirK/nirS* transcripts, suggesting an inhibitory effect in the expression of these genes (Afzal *et al.*, 2019; Broman *et al.*, 2019). We can say that appears to be true for our results of the mid-exponential experiment, but not for the late. Again, keeping in mind that the late-exponential experiment only has one replicate per treatment, and this behavior needs further confirmation.

Broman *et al.* (2019) demonstrated that cadmium might increase N_2 production. An increase in N_2 production by denitrification cannot happen without *nosZ* expression. In the late-exponential experiment, we saw there was a higher *nosZ* relative expression, compared to the *nirK* relative expression. Also, we encountered higher background levels of N_2O in the cadmium treatment, although they are still low values when compared to the mid-exponential experiment results. So, we can imagine that there could have been a stimulated reduction of N_2O, by stimulation of *nosZ* expression or effect on the enzyme after transcription, increasing N_2 production, in this late exponential phase of bacterial growth.

Overall, similarly to net N_2O production results, the results for *nirK* and *nosZ* relative expressions between mid and late-exponential experiments seem to be opposite. The results for *nirK* and *nosZ* relative expressions strongly support net N_2O production assessments.

Concluding Remarks

This dissertation led us to unveil new understandings on the cadmium effect on the net N_2O production of deep-sea bacteria. The methodological approach gave rise to an extensive discussion that ended in the refutation of our hypothesis – that cadmium would have an impact on *Shewanella loihica* PV-4 response, leading to higher net N_2O production.

Shewanella loihica PV-4 has demonstrated curious results on net N_2O production under cadmium treatment, appearing to have different responses when this metal is present in media. Having in mind that mid-exponential and late-exponential growing bacterial responses are different, my hypothesis is not true for the mid-exponential growth of *S. loihica* PV-4. However, found evidence and further work on the late-exponential phase might support that hypothesis. Moreover, net N_2O production results were supported by *nirK* and *nosZ* relative expression measurements, leading us to trust in this methodological approach, and to believe that gene expression regulation may be critical to predict cadmium impacts on net N_2O production. Either in the mid-exponential experiment, where cadmium appears to inhibit net N_2O production, or in the late-exponential experiment, where cadmium might increase N_2O production, this implies that the nitrogen cycle can be altered by cadmium exposure in marine environments.

Thalassospira indica PB8B appeared to be a good candidate for further experiments, possibly enabling similar experiments that can broad our knowledge on cadmium effect on the net N_2O production of deep-sea bacteria.

Overall, our findings highlight the importance of expanding our understanding on the environmental risks of deep-sea mining, an anthropogenic activity that can disturb microbial communities and function.

Future work

It is highly important that we expand our understanding on the environmental risks of deep-sea mining and its potential effects on deep-sea bacteria and benthic microbial communities.
Practical future work could include more replication of the late-exponential experiment, and replication of both experiments with *Thalassospira indica* PB8B and *Lutibacter profundi* LP1 to compare and understand if our results are transverse to other deep-sea isolates. I believe it would be very interesting to do similar and adapted experiments with pressure and with deep-sea sediments to study potential metal impacts in deep-sea bacterial communities, possibly bringing us closer to the reality of that distant habitat.
The MIDFun project will continue in the DeepResist project with the overarching goal to evaluate the impacts of metal exposure on the resistance and denitrifying transcriptomes in deep-sea conditions.

Appendix A

RNA purity check with recA

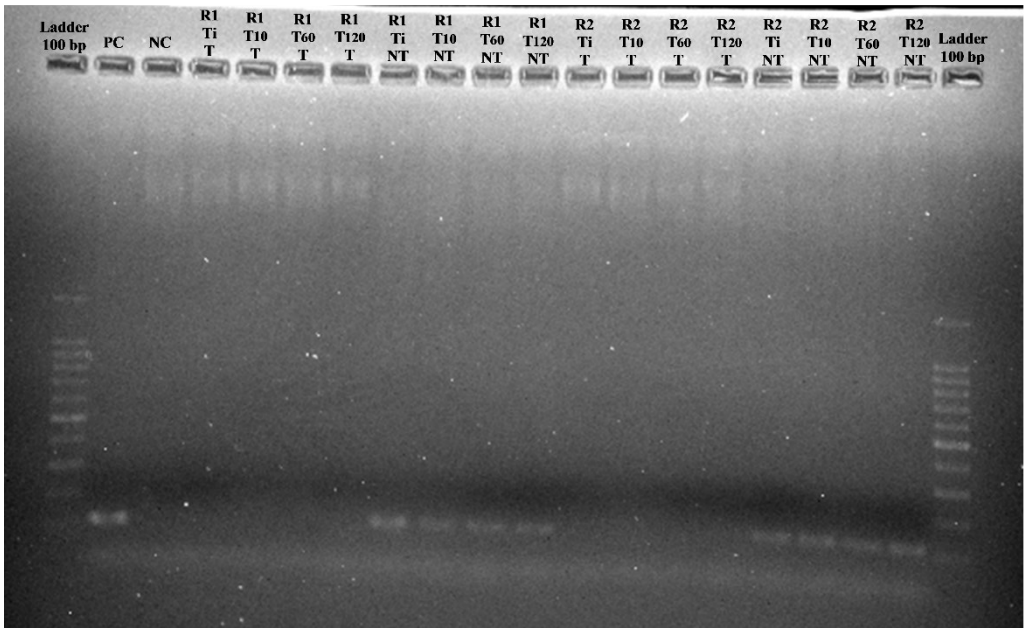

Figure A.1: Agarose gel photograph from RNA purity check with *reA* from experiment A. Wells are annotated for better comprehension. Legend: Ladder 100bp – ladder with 100 base pairs; PC – positive control; NC – negative control; R# - reactor 1 or 2; T# - time of sampling; T – treated samples; NT – non-treated sample for comparison.

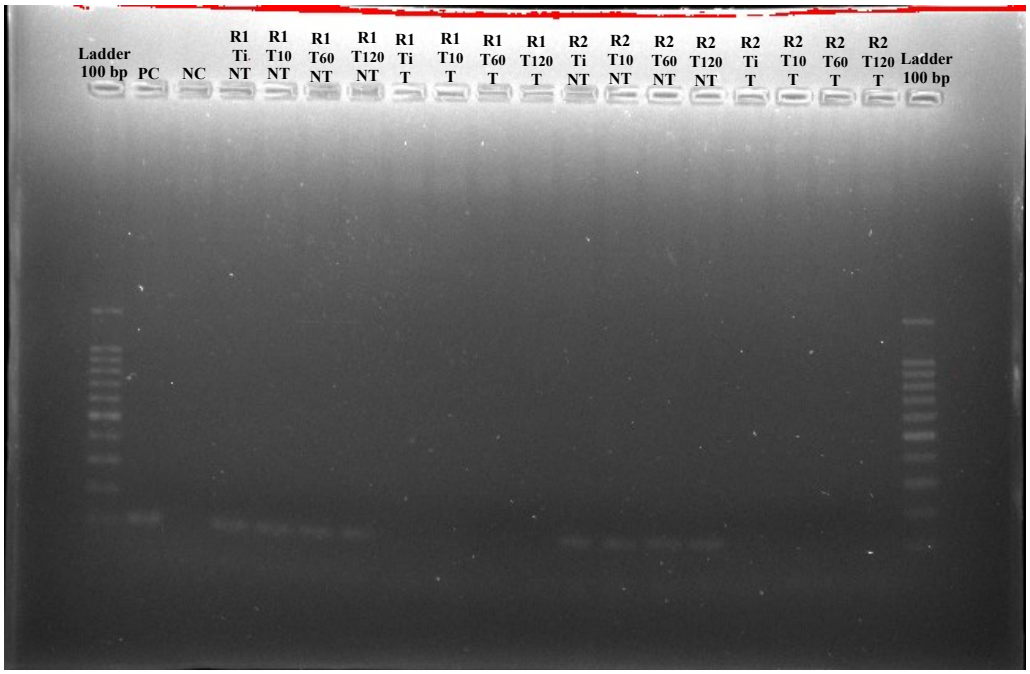

Figure A.2: Agarose gel photograph from RNA purity check with *reA* from experiment B. Wells are annotated for better comprehension. Legend: Ladder 100bp – ladder with 100 base pairs; PC – positive control; NC – negative control; R# - reactor 1 or 2; T# - time of sampling; T – treated samples; NT – non-treated sample for comparison.

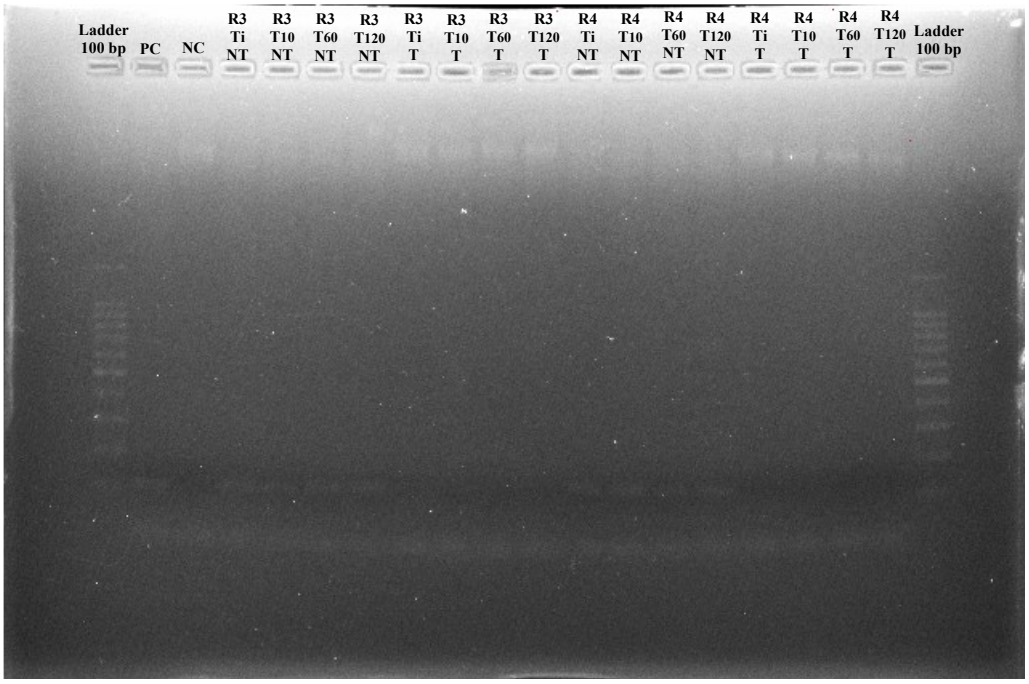

Figure A.3: Agarose gel photograph from RNA purity check with *reA* from experiment B. Wells are annotated for better comprehension. Legend: Ladder 100bp – ladder with 100 base pairs; PC – positive control; NC – negative control; R# - reactor 3 or 4; T# - time of sampling; T – treated samples; NT – non-treated sample for comparison.

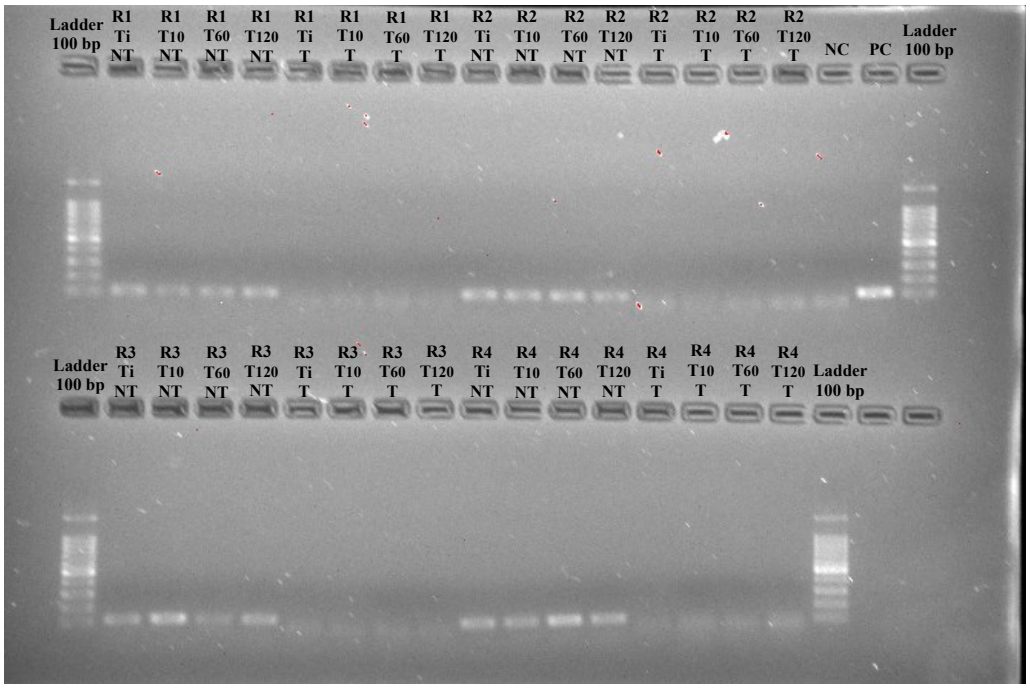

Figure A.4: Agarose gel photograph from RNA purity check with *reA* from experiment C. Wells are annotated for better comprehension. Legend: Ladder 100bp – ladder with 100 base pairs; PC – positive control; NC – negative control; R# - reactor 1, 2, 3 or 4; T# - time of sampling; T – treated samples; NT – non-treated sample for comparison.

Appendix B

Tests for data normality of the mid-exponential experiment – Shapiro-Wilk

Table B.1: Shapiro-Wilk test of normality for each treatment of the variables *nirK* relative expression, *nosZ* relative expression, and N_2O flux.

Tests of Normality[a,c,d]

		Kolmogorov-Smirnov[b]			Shapiro-Wilk		
	Treatment	Statistic	df	Sig.	Statistic	df	Sig.
nirK_relative_expression	Cadmium	.297	3	.	.917	3	.441
	Control	.286	3	.	.930	3	.490
nosZ_relative_expression	Cadmium	.244	3	.	.971	3	.676
	Control	.196	3	.	.996	3	.878
N2O_flux	Cadmium	.	3	.	.	3	.
	Control	.356	3	.	.818	3	.157

a. There are no valid cases for nirK_relative_expression when Treatment = .000. Statistics cannot be computed for this level.

b. Lilliefors Significance Correction

c. There are no valid cases for nosZ_relative_expression when Treatment = .000. Statistics cannot be computed for this level.

d. There are no valid cases for N2O_flux when Treatment = .000. Statistics cannot be computed for this level.

The statistical analysis was performed to a significance of 5%. Therefore, when sig.>0,05, we accept the null hypothesis, acknowledging that the data follows a normal distribution.

T-test for independent samples of the mid-exponential experiment

Table B.2: T-test for independent samples to evaluate the significance of the effect of the treatment, cadmium or control, on the *nirK* relative expression, *nosZ* relative expression, and N_2O flux.

Independent Samples Test

		Levene's Test for Equality of Variances		t-test for Equality of Means							
						Significance		Mean	Std. Error	95% Confidence Interval of the Difference	
		F	Sig.	t	df	One-Sided p	Two-Sided p	Difference	Difference	Lower	Upper
nirK_relative_expression	Equal variances assumed	9.413	.037	-1.473	4	.107	.215	-123.595000	83.901636	-356.543287	109.353287
	Equal variances not assumed			-1.473	2.002	.139	.278	-123.595000	83.901636	-484.201070	237.011070
N2O_flux	Equal variances assumed	4.284	.093	-1.366	5	.115	.230	-2.307750	1.689951	-6.651908	2.036408
	Equal variances not assumed			-1.616	3.000	.102	.205	-2.307750	1.428270	-6.853141	2.237641
nosZ_relative_expression	Equal variances assumed	3.671	.128	-5.413	4	.003	.006	-9.389000	1.734629	-14.205103	-4.572897
	Equal variances not assumed			-5.413	2.068	.015	.030	-9.389000	1.734629	-16.620937	-2.157063

The statistical analysis was performed to a significance of 5%. Therefore, when sig.>0,05, we accept the null hypothesis, acknowledging that there are no significant differences between treatments.

Appendix C

Standard curve for cadmium quantification in experiments A and B

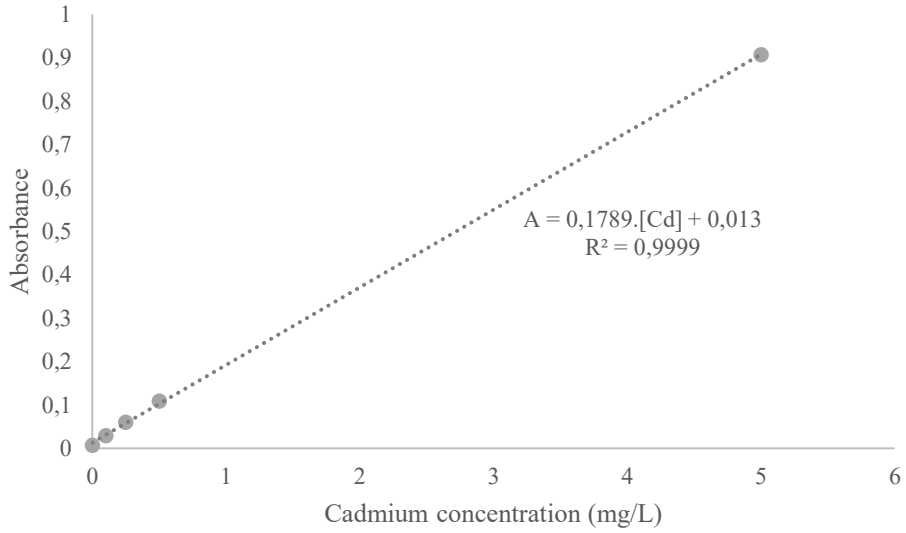

Figure C.1: Standard curve and linear regression for cadmium quantification in samples from experiments A and B.

Lower measured standard concentration = 0,1 ppm

Considered limit of detection for experiments A and B = 0,05 ppm

Standard curve for cadmium quantification in experiment C

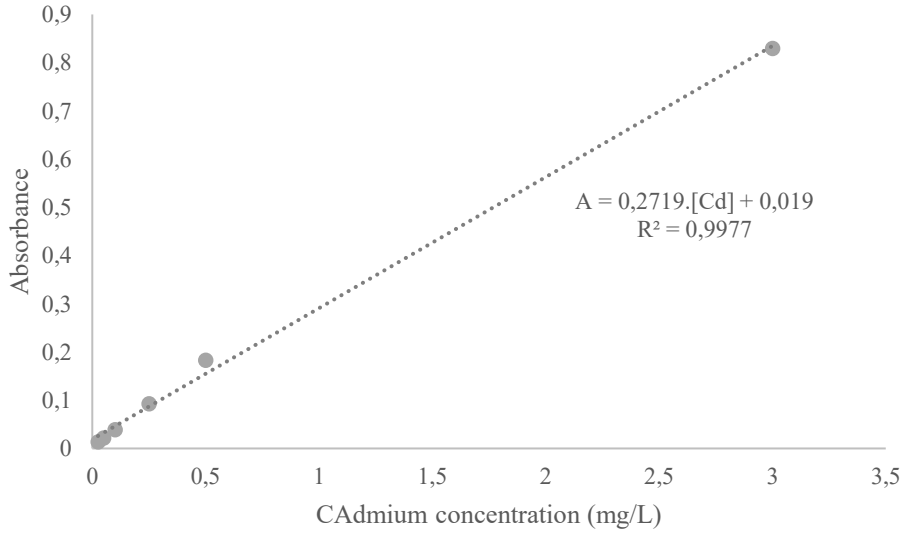

Figure C.2: Standard curve and linear regression for cadmium quantification in samples from experiment C.

Lower measured standard concentration = 0,025 ppm

Considered limit of detection for experiment C = 0,0125 ppm

References

Afzal, M. *et al.* (2019) 'The negative impact of cadmium on nitrogen transformation processes in a paddy soil is greater under non-flooding than flooding conditions', *Environment International*, 129, pp. 451–460. doi: https://doi.org/10.1016/j.envint.2019.05.058.

Arévalo-Martínez, D. L. *et al.* (2015) 'Massive nitrous oxide emissions from the tropical South Pacific Ocean', *Nature Geoscience*, 8(7), pp. 530–533. doi: 10.1038/ngeo2469.

Baker-Austin, C. and Dopson, M. (2007) 'Life in acid: pH homeostasis in acidophiles.', *Trends in microbiology*, 15(4), pp. 165–171. doi: 10.1016/j.tim.2007.02.005.

Bange, H. W. *et al.* (2019) 'A harmonized nitrous oxide (N2O) ocean observation network for the 21st century', *Frontiers in Marine Science*, 6(APR), pp. 1–10. doi: 10.3389/fmars.2019.00157.

Battaglia, G. and Joos, F. (2018) 'Marine N2O Emissions From Nitrification and Denitrification Constrained by Modern Observations and Projected in Multimillennial Global Warming Simulations', *Global Biogeochemical Cycles*, 32(1), pp. 92–121. doi: 10.1002/2017GB005671.

Bauer, S. L. M. *et al.* (2019) 'Profundibacter amoris gen. Nov., sp. nov., a new member of the roseobacter clade isolated from loki's castle vent field on the arctic mid-ocean ridge.', *International Journal of Systematic and Evolutionary Microbiology*, 69(4), pp. 975–981. doi: 10.1099/ijsem.0.003234.

Bauer, S. le M. *et al.* (2016) 'Lutibacter profundi sp. Nov., isolated from a deep-sea hydrothermal system on the arctic mid-ocean ridge and emended description of the genus lutibacter', *International Journal of Systematic and Evolutionary Microbiology*, 66(7), pp. 2671–2677. doi: 10.1099/ijsem.0.001105.

BBC (2021) *The world's forgotten greenhouse gas*. Available at: https://www.bbc.com/future/article/20210603-nitrous-oxide-the-worlds-forgotten-greenhouse-gas.

Breider, F. *et al.* (2019) 'Response of N2O production rate to ocean acidification in the western North Pacific', *Nature Climate Change*, 9(12), pp. 954–958. doi: 10.1038/s41558-019-0605-7.

Broman, E. *et al.* (2019) 'Denitrification responses to increasing cadmium exposure in Baltic Sea sediments', *Aquatic Toxicology*, 217(June), p. 105328. doi: 10.1016/j.aquatox.2019.105328.

Brown, A. *et al.* (2017) 'A comparative experimental approach to ecotoxicology in shallow-water and deep-sea holothurians suggests similar behavioural responses', *Aquatic Toxicology*,

191, pp. 10–16. doi: https://doi.org/10.1016/j.aquatox.2017.06.028.

Brown, A., Thatje, S. and Hauton, C. (2017) 'The Effects of Temperature and Hydrostatic Pressure on Metal Toxicity: Insights into Toxicity in the Deep Sea', *Environmental Science & Technology*, 51(17), pp. 10222–10231. doi: 10.1021/acs.est.7b02988.

Canfield, D. E., Glazer, A. N. and Falkowski, P. G. (2010) 'The evolution and future of earth's nitrogen cycle', *Science*, 330(6001), pp. 192–196. doi: 10.1126/science.1186120.

Chen, I.-M. A. *et al.* (2021) 'The IMG/M data management and analysis system v.6.0: new tools and advanced capabilities', *Nucleic Acids Research*, 49(D1), pp. D751–D763. doi: 10.1093/nar/gkaa939.

Chubukov, V. *et al.* (2014) 'Coordination of microbial metabolism', *Nature Reviews Microbiology*, 12(5), pp. 327–340. doi: 10.1038/nrmicro3238.

EPA United States Environmental Protection Agency (2022) *Understanding Global Warming Potentials*. Available at: https://www.epa.gov/ghgemissions/understanding-global-warming-potentials.

Freing, A., Wallace, D. W. R. and Bange, H. W. (2012) 'Global oceanic production of nitrous oxide', *Philosophical Transactions of the Royal Society B: Biological Sciences*, 367(1593), pp. 1245–1255. doi: 10.1098/rstb.2011.0360.

Gao, H. *et al.* (2006a) 'Shewanella loihica sp. nov., isolated from iron-rich microbial mats in the Pacific Ocean.', *International journal of systematic and evolutionary microbiology*, 56(Pt 8), pp. 1911–1916. doi: 10.1099/ijs.0.64354-0.

Gao, H. *et al.* (2006b) 'Shewanella loihica sp . nov ., isolated from iron-rich microbial mats in the Pacific Ocean', pp. 1911–1916. doi: 10.1099/ijs.0.64354-0.

Graf, D. R. H., Jones, C. M. and Hallin, S. (2014) 'Intergenomic comparisons highlight modularity of the denitrification pathway and underpin the importance of community structure for N2O emissions', *PLoS ONE*, 9(e114118).

Guan, N. and Liu, L. (2020) 'Microbial response to acid stress: mechanisms and applications', *Applied Microbiology and Biotechnology*, 104(1), pp. 51–65. doi: 10.1007/s00253-019-10226-1.

H.E.L Group (2022) *BioXplorer 400 | bench-top, parallel 4 bioreactor platform*. Available at: https://helgroup.com/products/bioreactors/bioxplorer-400/ (Accessed: 1 October 2022).

Hallin, S. *et al.* (2017) 'Genomics and Ecology of Novel N2O-Reducing Microorganisms', *Trends in Microbiology*, 26(1), pp. 43–55. doi: 10.1016/j.tim.2017.07.003.

Hallin, S. *et al.* (2018) 'Genomics and Ecology of Novel N2O-Reducing Microorganisms', *Trends in Microbiology*, 26(1), pp. 43–55. doi: 10.1016/j.tim.2017.07.003.

Hauton, C. *et al.* (2017) 'Identifying toxic impacts of metals potentially released during deep-sea mining-A synthesis of the challenges to quantifying risk', *Frontiers in Marine Science*, 4(NOV), pp. 1–13. doi: 10.3389/fmars.2017.00368.

Hutchins, D. A. and Capone, D. G. (2022) 'The marine nitrogen cycle: new developments and global change', *Nature Reviews Microbiology*, 20(7), pp. 401–414. doi: 10.1038/s41579-022-00687-z.

IBM Corp. (2021) 'IBM SPSS Statistics for Windows, Version 28.0.' Armonk, NY: IBM Corp.

J., J. D. *et al.* (2014) 'Undocumented water column sink for cadmium in open ocean oxygen-deficient zones', *Proceedings of the National Academy of Sciences*, 111(19), pp. 6888–6893. doi: 10.1073/pnas.1402388111.

Kumar, S., Stecher, G. and Tamura, K. (2015) 'MEGA7: Molecular Evolutionary Genetics Analysis version 7.0. Molecular Biology and Evolution'.

Kuypers, M. M. M., Marchant, H. K. and Kartal, B. (2018) 'The microbial nitrogen-cycling network', *Nature Reviews Microbiology*, 16(5), pp. 263–276. doi: 10.1038/nrmicro.2018.9.

Liu, Yang *et al.* (2016) 'Thalassospira indica sp. nov., isolated from deep seawater.', *International journal of systematic and evolutionary microbiology*, 66(12), pp. 4942–4946. doi: 10.1099/ijsem.0.001449.

Liu, Yuan *et al.* (2016) 'Abundance, composition and activity of denitrifier communities in metal polluted paddy soils', *Scientific Reports*, 6(March 2015), pp. 1–11. doi: 10.1038/srep19086.

Long, E. R. *et al.* (1995) 'Incidence of adverse biological effects within ranges of chemical concentrations in marine and estuarine sediments', *Environmental Management*, 19(1), pp. 81–97. doi: 10.1007/BF02472006.

Magalhães, C. *et al.* (2007) 'Impact of trace metals on denitrification in estuarine sediments of the Douro River estuary, Portugal', *Marine Chemistry*, 107(3), pp. 332–341. doi: https://doi.org/10.1016/j.marchem.2007.02.005.

Mason, O. U. *et al.* (2009) 'Prokaryotic diversity, distribution, and insights into their role in biogeochemical cycling in marine basalts', *ISME Journal*, 3(2), pp. 231–242. doi: 10.1038/ismej.2008.92.

Molina, L. *et al.* (2019) 'Pseudomonas putida KT2440 metabolism undergoes sequential modifications during exponential growth in a complete medium as compounds are gradually consumed', *Environmental Microbiology*, 21(7), pp. 2375–2390. doi: 10.1111/1462-2920.14622.

Mosier, A. C. and Francis, C. A. (2010) 'Denitrifier abundance and activity across the San

Francisco Bay estuary', *Environmental Microbiology Reports*, 2(5), pp. 667–676. doi: 10.1111/j.1758-2229.2010.00156.x.

Mullen, M. D. *et al.* (1989) 'Bacterial sorption of heavy metals', *Applied and Environmental Microbiology*, 55(12), pp. 3143–3149. doi: 10.1128/aem.55.12.3143-3149.1989.

National Center for Biotechnology Information (NCBI) (1988) *Bethesda (MD): National Library of Medicine (US), National Center for Biotechnology Information*.

Nguyen, J. *et al.* (2021) 'A distinct growth physiology enhances bacterial growth under rapid nutrient fluctuations', *Nature Communications*, 12(1). doi: 10.1038/s41467-021-23439-8.

Orcutt, B. N. *et al.* (2020) 'Impacts of deep-sea mining on microbial ecosystem services', *Limnology and Oceanography*, 65(7), pp. 1489–1510. doi: 10.1002/lno.11403.

Pajares, S. and Ramos, R. (2019) 'Processes and Microorganisms Involved in the Marine Nitrogen Cycle: Knowledge and Gaps', *Frontiers in Marine Science*, 6(November). doi: 10.3389/fmars.2019.00739.

Petersen, S. *et al.* (2016) 'News from the seabed – Geological characteristics and resource potential of deep-sea mineral resources', *Marine Policy*, 70, pp. 175–187. doi: https://doi.org/10.1016/j.marpol.2016.03.012.

Rocha, D. J. P., Santos, C. S. and Pacheco, L. G. C. (2015) 'Bacterial reference genes for gene expression studies by RT-qPCR: survey and analysis', *Antonie van Leeuwenhoek, International Journal of General and Molecular Microbiology*, 108(3), pp. 685–693. doi: 10.1007/s10482-015-0524-1.

Saide, A., Lauritano, C. and Ianora, A. (2021) 'A Treasure of Bioactive Compounds from the Deep Sea.', *Biomedicines*, 9(11). doi: 10.3390/biomedicines9111556.

Sakadevan, K., Zheng, H. and Bavor, H. J. (1999) 'Impact of heavy metals on denitrification in surface wetland sediments receiving wastewater', *Water Science and Technology*, 40(3), pp. 349–355.

Salgado, P. *et al.* (2014) 'Salinity as a regulator of DMSP degradation in Ruegeria pomeroyi DSS-3', *Journal of Microbiology*, 52(11), pp. 948–954. doi: 10.1007/s12275-014-4409-1.

Sánchez-Clemente, R. *et al.* (2018) 'Study of pH Changes in Media during Bacterial Growth of Several Environmental Strains', p. 1297. doi: 10.3390/proceedings2201297.

Semedo, M. *et al.* (2018) 'Antibiotic effects on microbial communities responsible for denitrification and N2O production in grassland soils', *Frontiers in Microbiology*, 9(SEP). doi: 10.3389/fmicb.2018.02121.

Semedo, M. *et al.* (2020) 'Differential expression of clade i and II N2O reductase genes in denitrifying Thauera linaloolentis 47LolTunder different nitrogen conditions', *FEMS*

Microbiology Letters, 367(24), pp. 1–6. doi: 10.1093/femsle/fnaa205.

Sharma, R. (2015) 'Environmental Issues of Deep-Sea Mining', *Procedia Earth and Planetary Science*, 11, pp. 204–211. doi: https://doi.org/10.1016/j.proeps.2015.06.026.

Stein, L. Y. (2011) 'Surveying N2O-producing pathways in bacteria.', *Methods in enzymology*, 486, pp. 131–152. doi: 10.1016/B978-0-12-381294-0.00006-7.

Xu, Y. and Morel, F. M. M. (2013) 'Cadmium in Marine Phytoplankton BT - Cadmium: From Toxicity to Essentiality', in Sigel, A., Sigel, H., and Sigel, R. K. O. (eds). Dordrecht: Springer Netherlands, pp. 509–528. doi: 10.1007/978-94-007-5179-8_16.

Ye, J. *et al.* (2012) 'Primer-BLAST: a tool to design target-specific primers for polymerase chain reaction.', *BMC bioinformatics*, 13, p. 134. doi: 10.1186/1471-2105-13-134.

Yoon, S. *et al.* (2015) 'Denitrification versus respiratory ammonification: Environmental controls of two competing dissimilatory NO 3-/NO 2-reduction pathways in Shewanella loihica strain PV-4', *ISME Journal*, 9(5), pp. 1093–1104. doi: 10.1038/ismej.2014.201.

Yoon, S., Sanford, R. A. and Löffler, F. E. (2015) 'Nitrite Control over Dissimilatory Nitrate/Nitrite Reduction Pathways in Shewanella loihica Strain PV-4.', *Applied and environmental microbiology*, 81(10), pp. 3510–3517. doi: 10.1128/AEM.00688-15.